AIRS

Algorithm Theoretical Basis Document

Level 1B

Part 1: Infrared Spectrometer

Version 2.1

15 December 1999

H. H. Aumann

Dave Gregorich, Steve Gaiser, Denise Hagan, Tom Pagano and Dean Ting

Jet Propulsion Laboratory
California Institute of Technology

File :ATBD1bir21p.doc

		Table of Contents		
1.		Introduction		7
2.		Infrared Spectrometer		
	2.1.	Instrument Overview		11
	2.2.	Calibration Devices		13
3.		Radiometric Calibration		
	3.1	Radiometric Calibration Equation		19
		1. Gain Calculation		19
		2. Space View Processing		20
		3. Scan Angle Correction (due to Polarization)		22
	3.2	Radiometric Error Estimation		24
		1. Scan Angle Emissivity Variation		25
		2. Radiometric Error Estimate Summary		29
		3. Detector Noise Estimation		31
4.		Spectral Calibration		
	4.1.	Conceptual Approach		33
	4.2.	Spectrometer Model		34
	4.3.	SRF centroid determination in orbit		37
		1. Spectral Feature Fitting		38
		2. Spectral Feature Selection		39
	4.4.	Spectral Calibration Error Estimation		42
5.		Spatial Calibration		45
6.		References		47
		Appendix		
		1. Concerns of the ATBD Review Team (July 1997)		49
		2. Dictionary of Abbreviations		55
		3. Radiometric Calibration Coefficients		57
		4. Polarization correction		61
		5. Radiance 1% offset to temperature offset conversion		65
		6. Channel Spectra		67
		7. Level 1b Validation		69

List of Tables

List of Figures

1. Introduction

The Level 1b Algorithm Theoretical Basis Document (ATBD) describes the theoretical bases of the algorithms used to convert the raw detector output (data numbers) from the Atmospheric Infrared Sounder (AIRS), the Advanced Microwave Sounding Unit (AMSU) and Humidity Sounder Brazil (HSB) to physical radiance units and, in the case of AIRS, perform in-orbit spectral calibrations. The description of the algorithms which convert the level 1b measurements to geophysical units is covered in the Level 2 ATBD.

The Level 1b ATBD for AIRS is divided into three parts:

- AIRS infrared spectrometer
- AIRS visible/near-infrared (VIS/NIR) channels
- AMSU/HSB Microwave channels.

This document is the ATBD for the level 1b processing of the AIRS infrared spectrometer. Level 1b algorithms perform the following functions:

1. conversion of scene measurements from engineering units to physical
2. estimation of detector noise,
3. estimation of the radiometric calibration accuracy
4. determination of the absolute spectral calibration and monitor spectral calibration stability.

Two reports related to the level 1b ATBD will issued in the year 2000:

1) The AIRS Spectrometer Calibration Report, which will include all data which define the AIRS instrument characteristics related to calibration. This report will include the tables of coefficients required by the level 1b software.

2) The AIRS In-orbit Calibration Plan, which will define test sequences to be executed in orbit to optimize instrument performance.

The most up-to-date description of the AIRS instrument development is given in Ref.1. The AIRS Functional Requirements Document (FRD) is in Ref. 2. The AIRS Calibration Plan (Ref.3), dated 14 November 1997, contains a description of the relevant parts of the AIRS instrument, calibration devices and calibration procedures for pre-launch characterization

of parameters needed by the level 1b algorithms. The AIRS Validation Plan (Ref. 4.) describes post-launch validation of level 1b data using floating buoys, radio sondes, satellite- and aircraft-borne instruments. The AIRS home page at JPL and the Earth Observing System (EOS) project office at GSFC, http://www-airs.jpl.nasa.gov and http://eospso.gsfc.nasa.gov, respectively, post latest version of these plans.

Version 2.10 of the level 1b ATBD includes a number of changes from Version 1.0

1) the AIRS instrument description, other than the description of calibration devices related to the level 1b algorithm, has been moved to the AIRS Calibration Plan; the infrared and the visible/near IR level 1b ATBD's are now separate documents;

2) comments from the ATBD level 1b review are addressed in the appendix; and

3) preliminary results of testing the AIRS Flight Unit (as of 15 October 1999) are included for the purpose of verifying the basis of the algorithms.

The AIRS flight model calibration and validation phase was completed by 15 November 1999.

1.1 Historical Perspective

The Atmospheric Infrared Sounder is a high spectral resolution IR spectrometer. AIRS, together with the Advanced Microwave Sounding Unit (AMSU) and the Microwave Humidity Sounder supplied by Brazil (HSB), is designed to meet the operational weather prediction requirements of the National Oceanic and Atmospheric Administration (NOAA) and the global change research objectives of the National Aeronautics and Space Administration (NASA). The AIRS flight model calibration started in November 1998 and was completed in November 1999. Integration onto the Aqua (formerly the EOS-PM1) spacecraft is scheduled to start in January 2000. The launch date for Aqua is 21 December 2000.

The High-resolution InfraRed Sounder (HIRS) and the Microwave Sounding Unit (MSU) on the National Oceanic and Atmospheric Administration (NOAA) polar orbiting satellite system have supported the National Weather Service (NWS) weather forecasting effort with global temperature and moisture soundings since the late 1970's. After analyzing the impact of the first ten years of HIRS/MSU data on weather forecast accuracy, the World Meteorological Organization in 1987 (Ref. 5) determined that global temperature and moisture soundings with radiosonde accuracy are required to significantly improve weather forecasts. Radiosonde accuracy is equivalent to profiles with 1 K rms accuracy in 1 km thick layers and humidity profiles with 20% accuracy in the troposphere. Advances in IR detector array and cryogenic cooler technology made this requirement realizable. AIRS is the product of this new technology. AIRS, working together with AMSU and HSB, forms a complementary sounding system for NASA's Earth Observing System to be launched in the year 2000.

The Interagency Temperature Sounder (ITS) Team, with representatives from NASA, NOAA, the University of Wisconsin and the Departmant of Defense (DOD) was formed in 1987 to convert the NOAA requirement for radiosonde accuracy retrievals to measurement requirements for an operational sounder. Instrument functional requirements established by this team in the areas of spectral coverage and resolution, calibration (radiometric and spectral), stability, spatial response (including alignment, uniformity, and measurement simultaneity), and sensitivity, became the basis of the AIRS Functional Requirements Document (Ref.2).

2. Infrared Spectrometer Description

2.1. Instrument Overview

The AIRS instrument and the devices and procedure used for the pre-launch calibration are described in the AIRS Calibration Plan, (Ref.3). In the following we describe those AIRS spectrometer design aspects which relate directly to the in-flight radiometric and spectral calibration activities and/or pre-launch calibration activities in support of the calibration software.

The AIRS instrument includes an infrared spectrometer and a visible light/near-infrared photometer. (The visible/near-IR photometer is discussed in Part 2 of the AIRS level 1b ATBD). The AIRS infrared spectrometer employs two multi-aperture slit and is pupil-imaging, with spectral coverage from 3.74 to 4.61 μm, from 6.20 to 8.22 μm, and from 8.8 to 15.4 μm. The nominal spectral resolution $\lambda/\Delta\lambda$ = 1200. The spectrum is sampled twice per spectral resolution element for a total of 2378 spectral samples. A diffraction grating disperses the radiation onto 17 linear arrays of HgCdTe detectors in grating orders 3 through 11.

Spatial coverage and calibration targets are provided by the scan head assembly, containing the scan mirror and calibrators. The scan mirror motor has two speed regimes: During the first 2 seconds it rotates at 49.5 degrees/second, generating a scan line with 90 ground footprints, each with a 1.1 degree diameter FOV. During the remaining 0.667 seconds the scan mirror finishes the remaining 261 degrees of a full revolution. Routine calibration related data are taken during this time. These consist of four independent views of Cold Space View (CSV), one view into the Onboard Blackbody Calibrator (OBC), one view into the Onboard Spectral Reference Source (OBS), and one view into a photometric calibrator for the VIS/NIR photometer.

The IR spectrometer is cooled by a two stage radiative cooler. The temperature of the spectrometer is fine-controlled by a temperature servo in combination with a 2.8 watt heater. The heater can raise the spectrometer temperature by about 7 degrees. The operating temperatures of the spectrometer is expected to be controlled at the start of the mission at 149K, 155K after about three years and 161K after about six years. Full radiometric and spectral calibrations will be carried out at all three set points. The temperature of the spectrometer is monitored with 6 fully redundant temperature sensors.

Stringent requirements on the stability of AIRS spectral calibration are achieved through the combination of three effects: The temperature control analog servo holds the spectrometer temperature constant at the set point to within 0.03K. The spectrometer was designed to be essentially a-thermal, i.e. the spectrometer optical bench, optical components and grating were machined from a single billet of specially annealed Aluminum. The spectrometer was designed

to have a thermal time constant of 20 hours. The high degree of stability of the AIRS spectrometer and its time constant have been verified during testing in the AIRS Test and Calibration Facility (ATCF).

The scan mirror rotates through 360 degree every 2.667 seconds. This produces data for one scan line with 90 footprints on the ground and 6 calibration related footprints. The scan mirror is cooled by radiative coupling to the cold IR spectrometer. Its temperature is monitored by a non-contacting sensor located at the base of the rotating shaft, about 6" from the scan mirror surface. The temperature gradient between the scan mirror surface and the temperature sensor is predicted to be less than 0.5K and temperature gradient across the scan mirror surface is less than 0.05K. Based on preliminary flight sensor test results in the thermal vacuum chamber, the scan mirror temperature is approximately 100K warmer than the spectrometer temperature. The scan mirror is coated with silver, overcoated with a protective layer of SiO_2 by Denton using a proprietary process. The scan mirror temperature, mirror angle (relative to nadir), emissivity, emissivity non-uniformity and polarization are part of the radiometric calibration algorithm.

The IR focal plane is cooled to 58 K by a Stirling/pulse-tube cryo-cooler and servo controlled at that temperature to within 0.01K. The Stirling/pulse-tube cryo-coolers are driven by separate electronics. The phase and amplitude of the compressor moving elements are designed to minimize vibration and to accurately control the temperature.

Signals from the detectors pass through onboard signal and data processing electronics, which perform signal amplification, radiation circumvention, offset subtraction, signal integration, and output formatting and buffering to the high rate science data bus. In addition, the AIRS instrument contains command and control electronics whose functions include communications with the satellite platform, instrument redundancy reconfiguration, the generation of timing and control signals necessary for instrument operation, and collection of instrument engineering and housekeeping data. Heat from the electronics is removed through coldplates connected to the spacecraft's heat rejection system.

2.2. Calibration Devices.

Routine calibration related data are taken while the scan mirror rotates from -49.5 degrees (relative to nadir) through 180 degrees (anti-nadir position) to +49.5 degrees. These data consist of four independent views of cold space (CSV), one view into the Onboard Radiometric Calibrator (OBC) source, one view into a Onboard Spectral reference source (OBS), and one view into a photometric calibrator for the VIS/NIR photometer. The AIRS spectrometer is pupil imaging, i.e. detectors are located at a pupil stop of the spectrometer optics (as opposed to the detectors being at a field stop, i.e. imaging the scene on the detectors). This insures that spatial

non-uniformity in the radiance emitted by the calibration source and/or the scene does not contribute to the radiometric calibration error.

Onboard Radiometric Calibrator (OBC): The OBC is a deep wedge cavity blackbody with a rectangular 5.7 cm by 9.5 cm clear aperture. The depth of the blackbody cavity is twice the diagonal of the clear aperture. The blackbody housing and cavity are made from beryllium to reduce its mass to 2 kg. The surface of the OBC wedge cavity is coated with paint with emissivity higher than 0.91. This allows multiple bounces of the light within the cavity. The OBC effective emissivity starts at 0.999 and degrades at end-of-life to no less than 0.993.

Four temperature sensors, T1..T4, monitor the temperature at key positions in the cavity surface to an accuracy of 0.1 K. T1 and T2 are located on the sloping part of the wedge, T3 is located on the vertical part of the wedge, and T4 is located at the outside aperture of the OBC. The OBC is analog servo controlled at 308.0 +/- 0.01K. The effective temperature of the OBC is calibrated using a NIST traceable external blackbody and related to a linear combination of T1..T4. This is discussed in Appendix 3.

The four temperature sensors in the OBC are fully redundant. If a temperature sensor is found to be outside the nominal limits, a flag is raised, indicating that the calibration accuracy may be compromised. Switch-over to the redundant sensor requires verification of the condition by the data monitoring team on the ground and uploading corrective action. Since the OBC temperature has been extremely stable during the entire ATCF testing, the level 1b algorithm continues with the data processing using the nominal OBC temperature.

Onboard Spectral reference source (OBS): A mirror coated with a thin film (about 100 microns thick) of Parylene is used as the On-Board Spectral reference source (OBS) for routine testing of spectrometer functionality pre-launch. Figure 2.2 shows the spectrum from two tests separated by 24 hours. The locations of usable spectral features are listed in Table 2.1. Although the spectral features are fairly broad, results from the thermal vacuum testing indicate that the OBS allows measurements of relative spectral shifts with repeatability of the order of 1% of the width of the spectral response function. The use of the spectral features of the OBS for in-orbit QA is under evaluation.

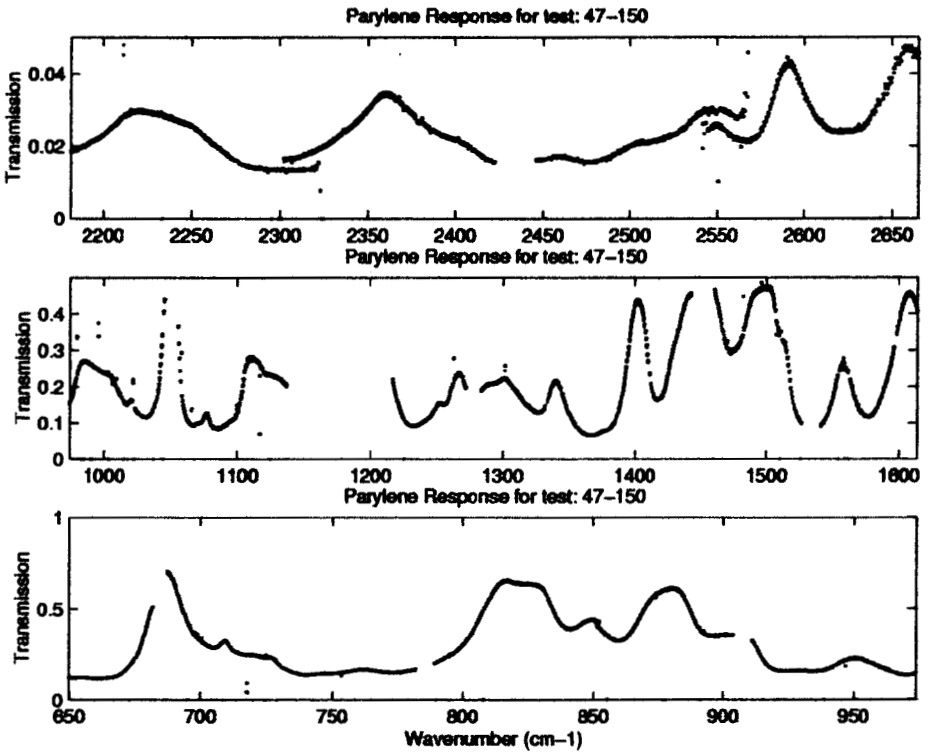

Figure 2.2. OBS spectra obtained during ATCF testing at the start and the end of the 24 hour orbital heat load simulation test.

Spectral Feature Location	Array location		Spectral Feature Location	Array location
709 cm^{-1}	M11		1233 cm^{-1}	M4d
970 cm^{-1}	M7		1327 cm^{-1}	M4c
1032 cm^{-1}	M6		1340 cm^{-1}	M3
1607 cm^{-1}	M4a		1402 cm^{-1}	M3
			1417 cm^{-1}	M3

Table 2.1. OBS Spectral Feature locations.

3. Radiometric Calibration

The required absolute radiometric calibration accuracy of each AIRS spectral channel, as stated in the AIRS Functional Requirements document (Ref.2.) , is the larger of 3% of the radiance or 4*NEN, over the full dynamic range of AIRS, where NEN is the Noise Equivalent Radiance. Since brightness temperature corrections or uncertainties are more useful radiance corrections or uncertainty for a temperature sounder, most of the discussion of radiance uncertainty is expressed as temperature uncertainty. A table in Appendix 5 lists the temperature change which corresponds to a 1% change in radiance as function of scene temperature.

The AIRS level 1b algorithm uses a basic radiometer calibration equation with additive correction terms. The AIRS spectrometer has 2378 spectral channels grouped in seventeen arrays. Each calibration operation is repeated for all 2378 spectral channels, somewhat loosely also referred to as 2378 detectors. Some minor differences between different detector arrays are called out when appropriate.

3.1. Radiometer Calibration Equation

Define for each frequency nu

$N = a.1 * W + a.2 * W^2 + a.3 * W^3 + \ldots + a.n * W^n$

where

N = radiance in physical units. For consistency with HIRS/2 instruments on the NOAA KLM series we have adopted units of $mW/m^2\ cm^{-1}$ sr for the AIRS level 1b spectral radiances.

DN.footprint = raw data number from a specific footprint after correcting for the ADC non-linearity using table lookup. There is only one redundant ADC for all detectors.

W.scene =DN.scene - DN.space

The first coefficient a.1 is commonly referred to as the "gain", G, for a linear radiometer. The coefficients are determined during the pre-launch calibration. Details and preliminary results are given in Appendix 3.

The radiance from the scene is conceptually given by

$N.scene = a.1 * W.scene + a.2 * W.scene^2 + a.3 * W.scene^3 + a.4 * W.scene^4$ Eq.3.-1

assuming that terms higher than 4-th order can be neglected.

The gain is determined orbit using the OBC. DN.space, the space views, are measured every scan line, but are smoothed over many scan lines to minimize noise. Some additive correction terms are required. This is discussed in the following.

3.1.1 In-orbit gain determination: In orbit we assume that the gain may be subject to some change from the pre-launch calibration, but that the higher order coefficients are unchanged. There are several reasons for an apparent change in the gain: T.obc.measured in orbit may be different than what was measured pre-launch, the system transmission may degrade due to contamination and/or the electronics gain may change due to component aging. The gain is calculated for every scan line using the known radiance output of the OBC

N.obc(nu) = e.obc(nu) * Planck(T.obc.measure + DT.obc, nu)

e.obc(nu) and DT.obc(nu) are determined pre-launch.

The gain is re-evaluate using

$$G = (N.obc - (a.2 * W.obc^2 + a.3 * W.obc.^3 + a.4 * W.obc.^4 \ldots..))/W.obc \qquad \text{Eq. 3-2}$$

The electronics in arrays M11 and M12 makes N.space > N.scene for any scene or calibration source temperature. This makes G<0. For all other arrays G>0.

The gain which is calculated using Eq.3-2 once per scan line is the instantaneous value of the gain. Eq. 3.1. uses the mean gain smoothed by averaging 100 (TBD) scan-line calibrations.

3.1.2. Space-View-Processing

The signal measured by AIRS viewing a ground target is the combination of the target radiance, the thermal emission from the AIRS instrument and electronics offset. The data number associated with a thermal emission and electronics offset is determined by means of the space views, DN.space. AIRS takes four space view measurements each scan line: S1, S2, S3 and S4. The space views occur while the AIRS boresight vector is between 68.6 and 112.2 degrees from nadir. The Earth horizon is at 61 degrees from nadir. These space view measurements are followed by a view of the blackbody. The cycle repeats every 2.67 seconds.

The four space views may be slight different due to the proximity of the Earth horizon for S1, and the underside of the spacecraft for S4. The lowest value will be selected in orbit as "the space view" to be used in the calibration algorithm. The current software uses #2 as "the space view". The level 1b software accumulates the following statistics on a routine basis: 1) the mean and standard deviation of the difference between S2 and S1, S2 and S3, and S2 and S4, and 2) the mean and standard deviation of change in each of the four space views during one scan line, DS1, DS2, DS3 and DS4, AVERAGE(DS2), STDEV(DS2), etc. This information is used to predict the value of the space view from one scan line to the next scan line (to guard against outliers) and to switch from one space view to another without impacting the calibration, if "the space view" should be contaminated , i.e. due the occasional presence of the moon.

In order to decrease the effect noise in individual space views, space view #2 data from a sliding window of about 100 (TBD) scan lines (about 5 minutes) are fitted as a function of time to a low order polynomial. The time-smoothed space views (#2) are used to calculate effective

space views S2s and S2e at the start and end of each scan line, respectively. Linear interpolation between S2s and S2e is used to evaluate DN.space at the time of the observation.

Occasionally (no more often than once per month) the Moon is located close to or in the AIRS field-of-view during the cold-space-view S2. The signal from the moon can be as large as 30% of full-scale. The exact algorithm for deciding if space view contamination has occurred has not been decided. Conceptually, if the Moon is within 3 degrees (TBD) of the space-view boresight based on ephemeris position and spacecraft orientation, then S2 is replaced by S3 - average(S3 - S2), assuming that S3 is the second lowest space view.

The analog output of each detector is periodically clamped by the electronics to voltage V_o at the end of the dwell period associated with viewing space view #2, but before space view #3. This event, referred to as the DCR ("DC Restore"), results in a discontinuity in S2. The discontinuity is due to changes in the detector background and electronics offset since the last DCR. The time of the DCR, which occurs every 1000 scan lines (TBD, a ground programmable period) is identified in the downlink data record. The level 1b software handles the step produced by the DCR by fitting S2 from the left and the right of the DCR time. V_o is set pre-launch to about 10% (TBD) of the dynamic range by a resistor, based on experience acquired during the calibration and characterization phase, as a zero offset of the analog-to-digital converter (ADC).

3.1.3. Scan Angle Dependent Radiometric Correction (due to Polarization)

The AIRS scan mirror adds a small amount of polarization to the scene radiance. This effect coupled with the polarization of the AIRS spectrometer produces a small radiometric offset that is scan angle dependent. The true scene radiance will then be the sum of the derived radiance using the normal calibration equation 3-1 plus a correction term that is scan angle dependent.

$$N_{true} = N.scene + dN_p(\delta)$$

In the following we give the algorithmic form of the correction term and show, based on the PFM test data, that the correction term decreases the polarization induced residual (i.e. error) to less than 0.1K.

3.1.3.1 Modeled Scan Angle Dependent Radiometric Correction

The radiometric correction term, dN_p, is

$$dN_p = p_r p_i \left\{ N \left[\cos 2(\delta - \alpha) - \left(1 - \frac{2N_s}{N_c} \right) \cos 2\alpha \right] - N_s \left[\cos 2(\delta - \alpha) + \cos 2\alpha \right] \right\} \qquad \text{Eq. 3-3}$$

where

δ = the scan mirror angle (derived from telemetry)
α = major polarization axis angle of the spectrometer (measured pre-flight) relative to nadir
p_r = polarization of the scan mirror (measured pre-flight)
p_i = polarization of the spectrometer (measured pre-flight)
N_s = radiance of a unit emissivity backbody at the temperature of the scan mirror (from telemetry)
N_c = the radiance of a unity emissivity blackbody at the temperature of the OBC (from telemetry)
N = the radiance of the scene (calculated neglecting polarization effects).

The radiometric correction therefore needs to be calculated and applied for every footprint of every channel of every scan. Eq.3-3 was validated during prelaunch calibration. Details are given in Appendix 4. The fit to the observed data is excellent. As shown in Figure 3.1. the correction terms are typically less than 0.5K . Based on the good correlation between measurements and model the expected residual errors of less than 0.1K.

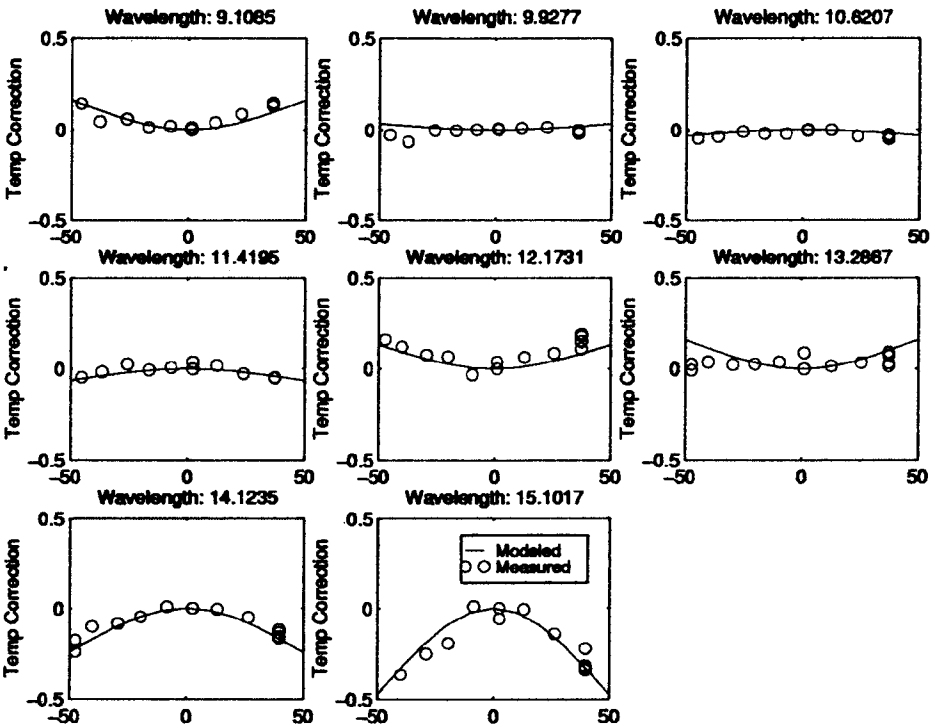

Figure 3.1. Scan angle dependent radiometric offset vs scan angle for the longest wavelength center module reference detectors. The small magnitude of the correction term and the excellent correlation between measurements and model suggest low residual errors.

3. 2. Radiometric Calibration Error Estimation

Radiometric terms which are not explicitly accounted for in the radiometric calibration equation, or which are due to uncertainties in the parameters used in the equation are error terms. Uncertainties in the level-1B products (offsets, gains, and radiances) are characterized as quasi-static error or time dependent error.

Quasi-static errors are assigned based on pre-launch calibration experience. They are a function of wavelength and signal amplitude.

Time-dependent and signal strength dependent errors are quantified based on two primary indicators. The first of these is the quality of the fits that are done to offset and gain. These quality indicators are in the form of rms deviations of data from a low order polynomial fit to a time series of measurements. The second quality indicator is the availability of calibration data. If good spaceview data are not usable over the desired smoothing interval (as will be the case due to the periodic presence of the Moon in the space view) the accuracy of the calibration will be degraded.

The combination of the following errors has to be considered in the total radiometric calibration accuracy estimate:

1) NIST transfer of the absolute calibration to the LABB
2) Transfer of the LABB calibration to the OBC
3) Residual non-linearity correction
4) Space view accuracy and space view time interpolation error
5) Residual polarization scan angle dependent error
6) Scan angle dependent emissivity (start and end of life).

The scan angle dependent emissivity correction term is the only term in the radiometric calibration equation which is explicitly neglected in the AIRS level 1b algorithm.

3.2.1. Scan angle dependent scan-mirror emissivity.

The AIRS scan mirror emissivity (averaged over the AIRS spectral coverage) is 0.015, with an estimated rms variation of less than 0.0005. The AIRS radiometric calibration uses different parts of the scan mirror for the scene, the space view and the OBC view.

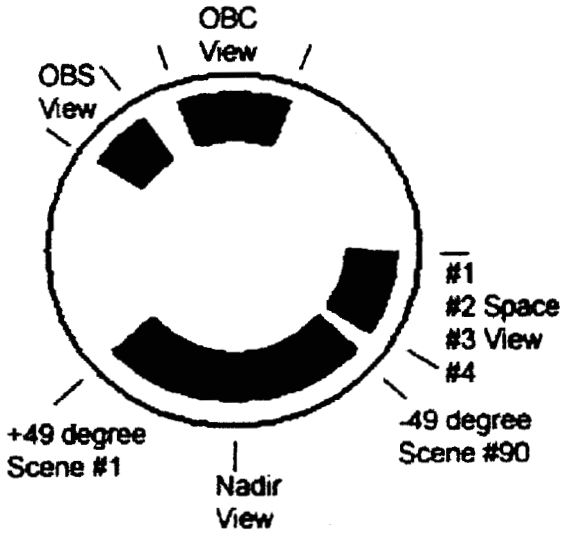

Figure 3.2 The scan mirror rotates through 360 degree every 2.667 seconds, producing one scan line with 90 footprints on the ground and 6 calibration related footprints. Different parts of the scan mirror (highlighted in black for arrays M11 and M12) are used for calibration views and scene views.

Arrays M5 through M12 us the outer part of the scan mnirror, while arrays M1 through M4 use the center part. During the pre-launch calibration a scan angle dependent correction term is measured which includes scan angle dependent emissivity effects. However, during storage and/or after some time in orbit the emissivity of the scan mirror may differ from the pre-launch calibration values. It is estimated that after five years on orbit (nominally the End of Life, EOL) the layer of molecular contaminants on the scan mirror will be 100A thick, increasing its emissivity by 0.01 to 0.025. Since the mirror is protected inside the rotating barrel baffle, there is no preferred area of exposure to deposits. We therefore expect the 100A thick layer to be very uniform in thickness. The following section gives the derivation of the correction term and a worst case estimate of the magnitude, assuming a 100A thick layer with a 10% variation in contaminant thickness. This variation in emissivity would cause an rms emissivity variation of 0.001. The analysis shows that the resulting the emissivity correction term can be neglected.

1. Derivation of the correction term.

We express true radiance from the scene, N(δ), as the sum of the scan angle emissivity independent term , No, a correction term, ΔN(δ),

$$N(\delta) = No + \Delta N(\delta).$$

Assume that the scan mirror emissivity seen by a detector at scan angle δ relative to nadir is e(δ). There are 90 scene views at scanangles $-49 < \delta < +49$ degrees, space view S2 occurs at scan angle δ=s, and the OBC is viewed at scan angle δ=b. The reflectivity of the scan mirror is r(δ)=1-e(δ). The signal N(δ) from the scene then gives the output:

$$V(\delta) * G = N(\delta)*r(\delta) + e(\delta)*N(s) + Xo$$

The space view signal due to the scan mirror emissivity and other background or electronic offset signals, Xo, is

$$V(s) * G = N(s)*e(s) + Xo$$

and the view at the calibration blackbody produces:

$$V(b) * G = N(b)*(1-e(b)) + e(b)*Ns + Xo.$$

These equation can be combined as

$$\frac{V(\delta)-Vs}{Vb-Vs} = \frac{N(\delta)*(1-e(d)) + Ns(e(d)-e(s))}{Nb*(1-e(b)) + Ns(e(b)-e(s))} \qquad \text{Eq. 3-4}$$

Since $e(\delta)<<1$ and $Ns * (e(b)-e(s)) / Nb << 1$ with the cold scan mirror this equation can be simplified to

$$\Delta N(\delta) = Ns * (e(s)-e(\delta)) - No * (e(b)-e(\delta)). \qquad \text{Eq. 3-5}$$

As a check of the equations, note that if the scan mirror emissivity is uniform, i.e. $e(\delta)=e(s)=e(b)$, then $\Delta N(\delta)=0$, i.e. the correction term vanishes for all δ.

2. Estimate of the magnitude of the correction term DN.

The panel in Figure 3.3. shows the assumed conditions for the change between the pre-launch/begin of life and end of life conditions with respect to scan mirror temperature, average emissivity of the scan mirror for scene view, OBC view and space view, respectively, based on the assumed worst case 0.001 variation of the scan mirror emissivity.

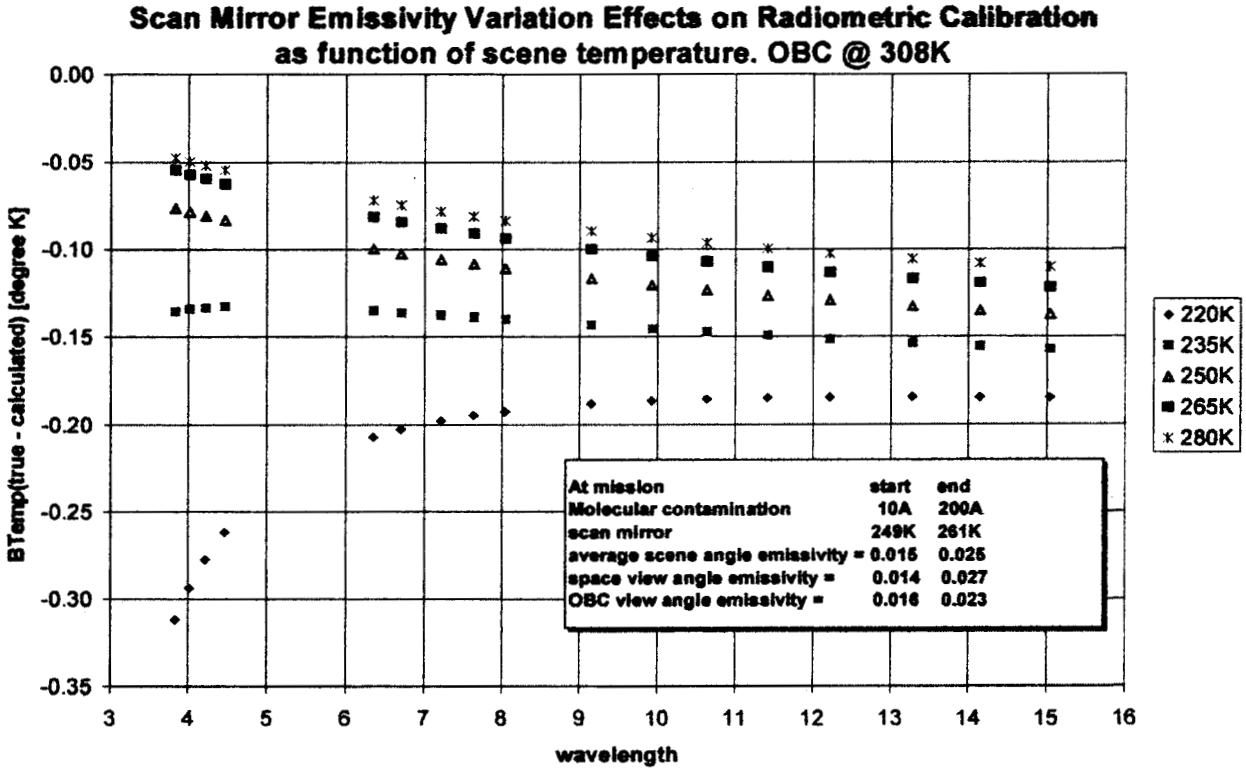

Figure 3.3. Effect of scan mirror emissivity variation on calibration between characterizion pre-launch and end-of-life (which is degraded by contamination) for a worst case emissivity variation of 0.001. The differences at temperatures above 235K in the 0.05 to 0.1K class.

Since retrievals are carried out in terms of brightness temperatures, we express the scan mirror emissivity variation dependent correction term ΔN as a temperature correction ΔT. This is

shown in Figure 3.3. as function wavelength and scene temperature . At brightness temperatures of 235 K and warmer the magnitude of the correction term is less than 0.15K. At lower temperatures the correction is somewhat larger. The AIRS level 1b processing neglects this term. The term is therefore included it in the overall radiometric uncertainty estimate.

3.2.2. Radiometric Error Estimate Summary

The radiometric error depends on the spectral region and the scene temperature. Table 3.1. presents a summary of the radiometric calibration error estimate based on quick-look analysis of the final calibration data for the midpoint of each array at a scene temperature of 250K. The estimate does not include the absolute NIST calibration error. At the start of the mission (highlighted area) the estimated error ranges from 012K to 0.26K in brightness temperature. The equivalent flux error range is 0.35% – 0.74%. With an additional estimated NIST absolute calibration uncertainty of 1%, the absolute calibration accuracy is considerable better than the requirement. There is a slight additional degradation if the worst case estimate for scan mirror contamination after five years is included. A complete analysis with respect to the requirements will be completed when the calibration data have been fully analyzed.

Table 3.1. Radiometric Calibration Error Estimate (1) at T = 250 degree K

array	array mean	LABB calibration via NIST	308K OBC calibration via LABB	residual non-linearity fit at T	space view inter-polation	residual scan angle dependent correction	BOL scan mirror emissivity variation	[illegible]	[illegible] total % of flux	EOL scan mirror emissivity variation	End of mission total degree K	total % of flux
		error deg K	error deg K	error deg K	error deg K	error deg K	error deg K	[illegible]	[illegible] RSS (1)	error deg K	RSS error	RSS (1)
M1a	3.82665	0.05	0.05	0.05	0.05	0.05	0.075	[illegible]	0.74	0.15	0.19	1.17
M2a	4.21955	0.05	0.05	0.05	0.05	0.05	0.07	[illegible]	0.67	0.14	0.18	1.00
M1b	4.01245	0.05	0.05	0.05	0.05	0.05	0.07	[illegible]	0.70	0.14	0.19	1.09
M2b	4.4678	0.05	0.05	0.05	0.05	0.05	0.06	[illegible]	0.63	0.13	0.18	0.92
M4a	7.20625	0.05	0.05	0.05	0.05	0.05	0.05	[illegible]	0.39	0.09	0.15	0.48
M4b	6.34685	0.05	0.05	0.05	0.05	0.05	0.05	[illegible]	0.46	0.10	0.16	0.57
M3	6.7002	0.05	0.05	0.05	0.05	0.05	0.05	[illegible]	0.42	0.09	0.15	0.53
M4c	7.6333	0.05	0.05	0.05	0.05	0.05	0.05	[illegible]	0.37	0.09	0.15	0.45
M4d	8.04025	0.05	0.05	0.05	0.05	0.05	0.04	[illegible]	0.36	0.08	0.15	0.42
M5	9.14345	0.05	0.1	0.1	0.05	0.1	0.04	[illegible]	0.49	0.08	0.21	0.53
M6	9.92	0.05	0.1	0.1	0.1	0.1	0.04	[illegible]	0.46	0.07	0.22	0.52
M7	10.63	0.05	0.1	0.1	0.1	0.1	0.04	[illegible]	0.46	0.07	0.22	0.49
M8	11.4108	0.05	0.1	0.1	0.1	0.15	0.03	[illegible]	0.49	0.07	0.25	0.51
M9	12.21405	0.05	0.15	0.1	0.1	0.15	0.03	[illegible]	0.50	0.07	0.27	0.52
M10	13.2723	0.05	0.15	0.1	0.1	0.15	0.03	[illegible]	0.47	0.07	0.27	0.48
M11	14.1455	0.05	0.15	0.05	0.05	0.15	0.03	[illegible]	0.38	0.06	0.24	0.40
M12	15.0336	0.05	0.15	0.05	0.05	0.15	0.03	[illegible]	0.37	0.06	0.24	0.38

(1) Absolute NIST calibration error not included

3.2. Detector noise estimation

The level 1b software routinely characterizes the gaussian noise amplitude and non-gaussian characteristics (if any) for each channel. This information is passed to the level 2 algorithm for use in the retrieval accuracy estimation.

1. Gaussian noise estimation

a) A byproduct of the smoothed gain calculation, defined as MEAN(V_{sc}-V_{ss}), is the STDEV(V_{sc}-V_{ss}) for a 100 (TBD) point scan-line window. The detector noise equivalent radiance is

$$NEN1=G * STDEV(V_{sc}-V_{ss})/root(2),$$

where root(2) accounts for noise in both the space view and the calibrator view.

b) An alternate estimate of the detector noise

$$NEN2= G * STDEV(DS2)/root(2).$$

STDEV(DS2) is defined in section 3.1.3. A selection between NEN1 and NEN2 will be based on an in-orbit evaluation of the stability of the measurement.

2. Non-gaussian noise estimation.

Based on ATCF test analysis the output, V_{ss}, observed for successive space views for each detector is predictable to an accuracy approaching the gaussian noise for most detectors. The level 1b software makes use of this fact for QA by predicting the space view data number, PV_{ss}. If (PV_{ss} - V_{ss})> k* STDEV(DS2), then the software assumes that some kind of transition occurred in the detector or the electronics. This is referred as a "pop" or "popcorn noise". The multiplier k tentatively set to 3 (TBD). The number of "pop's" per unit time element is included in the QA report. No space view smoothing occurs across a scan line where a "pop" was detected.

4. Spectral Calibration

"AIRS infrared spectral calibration" means determining how each infrared detector in the AIRS instrument responds to incident radiation of different wavelengths. This characterization is called the Spectral Response Function (SRF) of the detector. Determining the shape of these SRF's is a calibration task and therefore not part of the level 1b algorithms. SRF shape and position uncertainty and the effect on the accuracy of the upwelling spectrum calculated by the forward algorithm is is discussed in the L2 ATBD. Determining the spectral positions [centroids] of these SRF's is a the Level-1B task.

The AIRS spectrometer has a spectral resolution $R=\lambda/\delta\lambda$ nominally equal to 1200, where $\delta\lambda$ is a detector's full width at half its maximum response (FWHM). The Functional Requirements Document (FRD) calls for a knowledge of detector centroid frequencies (for each array element) to within 1% of $\delta\lambda$ at all times. These frequencies are not to vary by more than 5% over any 24 hour period. The FRD also demands knowledge of $\delta\lambda$ no worse than 1%.

4.1 Conceptual Approach and Justification

AIRS in-orbit infrared spectral calibration is absolute, using identified features at known spectral locations in observed upwelling radiance spectra. It is based primarily on three components:

1) Focal plane detector assembly models;
2) A spectrometer grating model; and
3) Upwelling radiance spectra [both measured and modeled].

The focal plane detector assembly models specify the position of each AIRS infrared detector on the focal plane assembly, relative to the other detectors. A different focal plane detector assembly model is used for each of the three spectrometer thermostat set-points (149K, 155K, and 161K).

The spectrometer grating model specifies the relation between detector SRF centroids and detector physical positions (relative to the grating and the imaging optics). This is discussed at greater length in section 4.2.

The radiance spectra [both modeled and measured] provide "tie-points," allowing determination of the absolute position of the focal plane detector assembly. This is discussed at greater length in section 4.3.

The underlying assumption allowing this approach is that, for a given instrument condition (spectrometer temperature and optics alignment), the focal plane detector assembly remains invariant. This assumption has been born out by three types of test performed pre-launch:

A) Detector response centroids were measured before and after acoustic and vibrational testing. Differences observed in detector SRF centroid (corresponding to 13% of $\delta\lambda$) were consistent with a shift of the focal plane assembly relative to the spectrometer optics, and showed no signs that the detectors moved within the focal plane assembly;

B) Detector response centroids were measured in both +1g and –1g environments (to estimate the magnitude of zero-g release effects). Differences observed in detector SRF centroids (corresponding to 3% of $\delta\lambda$) were consistent with a shift of the focal plane assembly relative to the spectrometer optics, and showed no signs that the detectors moved within the focal plane assembly;

C) Detector response centroids were measured repeatedly during an extended (24-hour) test simulating 14 day-night heating cycles. Again, differences observed in detector SRF centroids (this time corresponding to just 0.25% of $\delta\lambda$) were consistent with a shift of the focal plane assembly relative to the spectrometer optics, and again showed no sign that the detectors moved within the focal plane assembly.

4.2 Spectrometer Model

The AIRS spectral calibration relies on a spectrometer calibration model derived from the textbook grating equation

$$m*l = d * (\sin(a) + \sin(b)) \qquad \text{(Eq. 4-1)}$$

where

m = the grating order,
l = the wavelength,
d = the grating constant (the spacing between rulings on the grating),
a = the angle of incidence, and
b = the angle of diffraction.

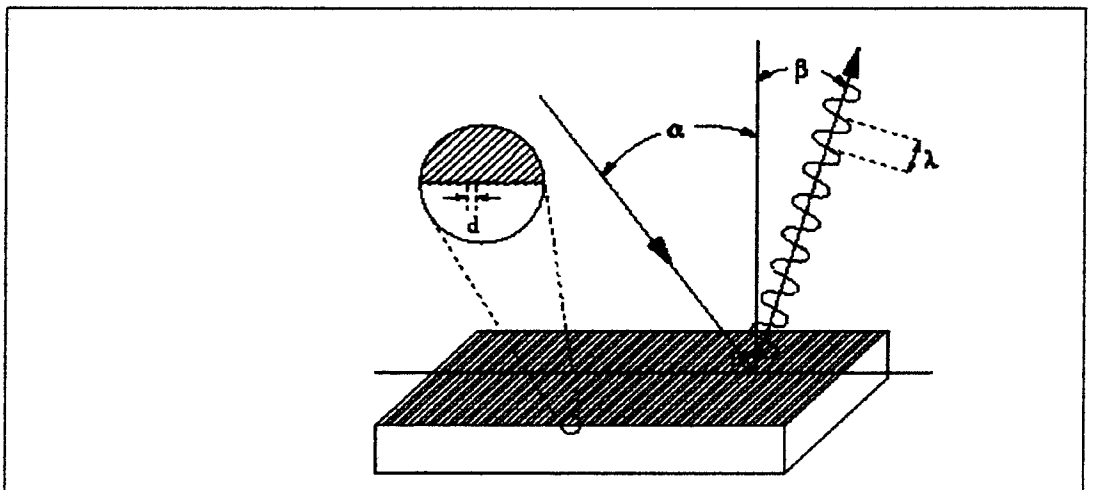

Figure 4-1 shows a schematic of a simple grating spectrometer with each of the five key model parameters, except grating order.

Figure 4-1 is a sketch of a simple grating spectrometer. The actual AIRS spectrometer is folded with a considerably more complicated layout, but the basic equation 4-1 applies. AIRS works in grating orders 3 (at the longest wavelengths) to 11 (at the shortest wavelengths). Through the use of two spectral bandpass filters for each detector array, one covering the spectrometer entrance slit, the other directly over each detector array, and geometric optics, each detector array is guaranteed to see radiation from only one grating order.

Thus for the a single detector array in the AIRS optical system, equation 4-1 can be rewritten (solving for l_i) as:

$$l\_i = d/m[\sin(a) + \sin(\arctan(((X\_0 + X\_i)/L)))] \qquad \text{(Eq. 4-2)}$$

where

l_i	= the wavelength of SRF centroid of the i'th detector,
d	= the grating constant,
m	= the grating order (for the detector array of interest),
a	= the angle of incidence (onto the grating),
X_0	= the distance [in the along-dispersed direction] from the center of the focal plane to the optical axis of the system,
X_i	= the distance [in the along-dispersed direction] to the i'th detector, from the center of the focal plane, and
L	= the optical pathlength from the focusing mirror to the focal plane.

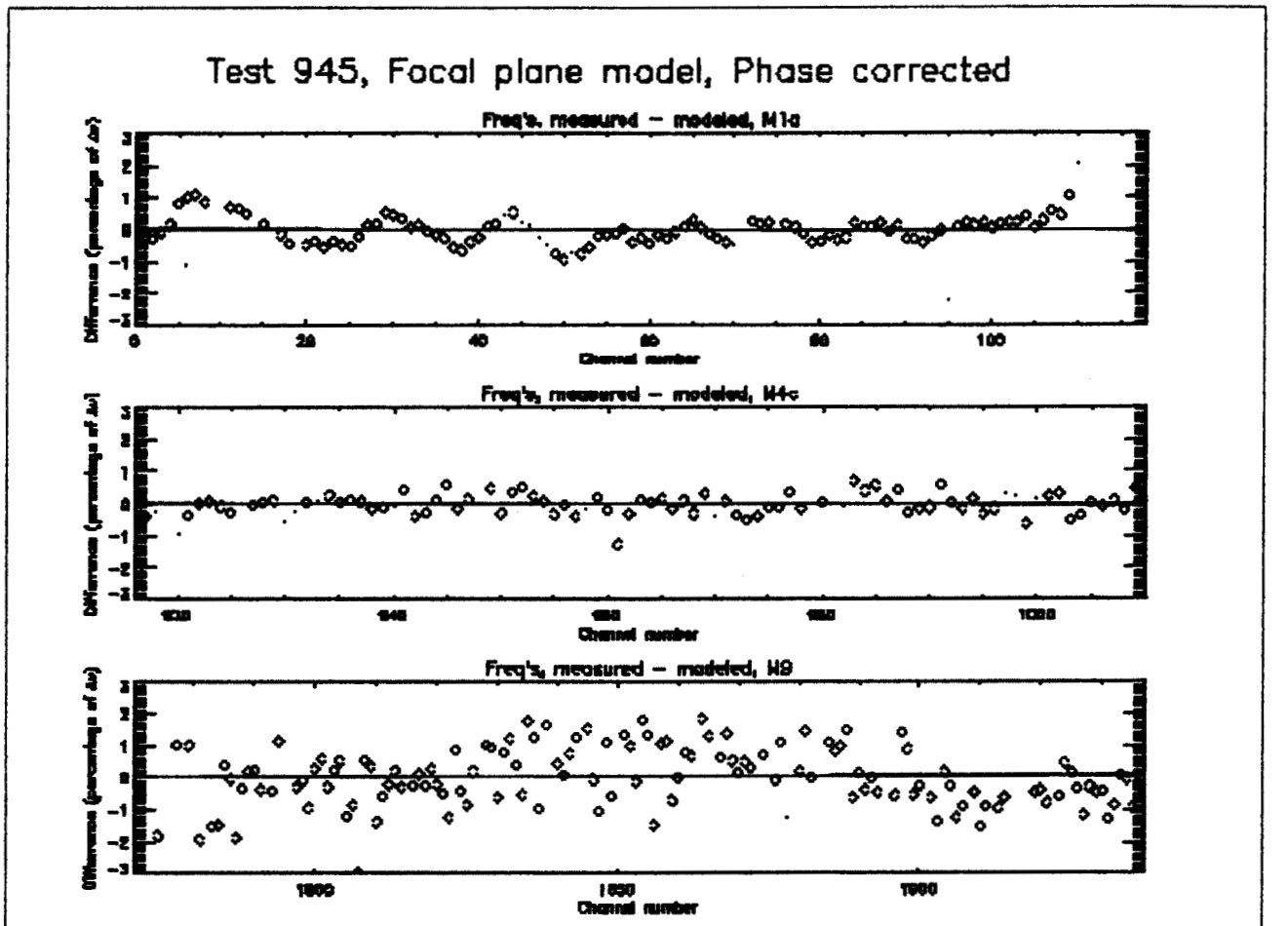

Figure 4-2 shows results of fitting observed SRF centroids from individual detectors to the spectrometer model for three representative arrays. Deviation of any one detector from the model is typically much less than 3% of the SRF width, the full scale of the plot.

The systematic patterns in the differences between model fit and individual channels shown in Figure 4-2, seen particulary clearly in the shortest wavelength array M1a (2553 – 2676 cm-1), are due to the presence of channel spectra (see Appendix 6). At the longer wavelengths (array M4c, 1283 cm-1 - 1338 cm-1, and array M9, 788 cm-1 - 851cm-1) the deviations are increasingly dominated by random noise in the measurements. In all cases, the RMS deviation of the model fit from the data is less than 1% of the FWHM.

Analysis of pre-launch spectral responses indicates that the focal plane detector assembly is not co-planar (or, more precisely, that the focal plane does not fall exactly on a [slightly non-planar] wavefront). These focal length differences are minute from detector to detector, but significant from array to array. Fortunately, as with the detector translational positions, pre-launch testing indicates that the observed relative focal length differences appear constant, for a given instrument thermal set-point. Expressing L as the mean focal length L_0 plus an array-dependent delta dL_k, we have (explicitly showing all dependences):

$$l\_i = d(T)/m(k)[\sin(a(k,T)) + \sin(\text{atan}((X\_0 + X\_i/(L\_0 + L(k,T)))))] \qquad \text{(Eq. 4-3)}$$

where

- l_i = the wavelength of the i'th detector,
- d(T) = the grating constant at spectrometer thermal set point T,
- m(k) = the order of detector array k,
- a(k,T) = the incidence angle on the grating for detector array k, at spectrometer thermal set point T,
- X_0 = the distance [in the along-dispersed direction] from the center of the focal plane to the optical axis of the system,
- X_i = the distance [in the along-dispersed direction] to the i'th detector, from the center of the focal plane, and
- L_0 = the nominal optical pathlength from the focusing mirror to the focal plane, and
- L(k,T) = the measured (pre-launch) difference between the nominal focal length to the k'th detector array and the nominal focal length, at spectrometer thermal set point T.

Values for the parameters d, m, a, X_i, and L were accurately determined during pre-launch calibration, leaving X_0 and L_0 to be determined in orbit as part of the level 1b algorithm. "Fitting the grating equation" then becomes a matter of determining L_0 and X_0. Once L_0 and X_0 have been chosen, equation 4-3 yields a calculated centroid wavelength for each detector.

Three precision screws in the Actuated Mirror Assembly (AMA) can be turned in flight, finely repositioning the focusing mirror. This permits in-flight control of L_0 and X_0. [The third degree of freedom controls the cross-dispersed imaging of the entrance slits onto the detector arrays.] During prelaunch alignment of the instrument, L_0 is set to an optimum distance (approximately equal to the on-axis focal length of the focusing mirror).

4.3 SRF Centroid Determination in Orbit

The in-orbit SRF centroid determination method can be summarized as:

A) Determine the positions (on the detector array assembly) at which a spectral feature is located; and

B) Select X_0 and L_0 in the grating spectrometer model (Eq. 4-3) to minimize the differences between the calculated wavelengths (from the grating spectrometer model) and the known, pre-determined wavelengths of the feature of interest.

These two steps, as well as the criteria for upwelling radiance feature selection, are described below.

4.3.1 Spectral Feature Fitting

The spectral features which have been selected are based on radiative transfer calculations with climatologically representative atmospheric conditions. Because radiative transfer in thermodynamically stable atmospheres is readily computable (good physics), and because

absorption/emission line positions and strengths are well measured (good spectroscopy), the locations of the selected spectral features are also extremely well known.

The method used to determine the position of each spectral feature is as follows:

a) First, obtain an observed upwelling radiance spectrum. In principle, every AIRS spectrum could be used for wavelength calibration. In practice, only those four observations nearest nadir will be used. Only spectra for the nadir location thus have to be stored. Furthermore, to increase signal-to-noise, only those footprints which are cloud-free (as determined by a spectral contrast criterion, on a feature-by-feature basis) will be used. Such near-nadir, cloud free radiance spectra will be accumulated for five minutes (actually interval TBD) and averaged. The tremendous thermal stability of the AIRS instrument, as measured pre-launch, allows us to do this, even as the instrument crosses the terminator.

b) Then select nominal values of X_0 and L_0 (and use the measured, pre-launch values of the other spectrometer grating model parameters) to calculate nominal frequencies (using equation 4-3) for some number of detectors (about 14, typically) spanning the feature of interest.

c) Sample the pre-calculated [modeled] upwelling radiance spectrum at those frequencies, using an appropriate climatology for the upwelling radiance spectrum.

d) Calculate new detector frequencies corresponding to shifting the focal plane (changing X_0) by +-5, 10, 15, 20, and 25 microns.

e) Sample the same [modeled] upwelling radiance spectrum at these ten sets of new frequencies.

f) Calculate the correlation coefficient between each of the eleven sampled radiance spectra and the observed radiance spectrum, using the Pearson algorithm (Ref. 7).

g) Fit a parabola to the observed correlation coefficients, and determine the location of the peak of the parabola.

The calculated position of the peak (in microns translation of X_0) is then added to the nominal position of the feature (determined pre-launch), yielding the observed position of the peak.

This procedure is carried out for each of the approximately 25 (TBD) chosen features, producing a set of 25 (TBD) frequency/position pairs (the frequencies of the features, like their nominal positions, are calculated once, pre-launch).

With these 25 (TBD) calculated positions (X_i's calculated from upwelling radiance spectra) and their corresponding 25 known wavelengths, values of L_0 and X_0 are found which minimize residuals between calculated and known frequencies, in a least-squares sense. The simplex search algorithm "Amoeba" (Ref. 7) is used to accomplish this.

With X_0 and L_0 determined by the fit, a new frequency set is obtained by applying equation 4-3 to all the X_i's. These calculated values are the "measured frequencies" reported to Level-2.

4.3.2 Spectral Feature Selection

Spectral features to which to fit observed radiance must satisfy a number of criteria:

1) Because these "tie-points" anchor the fit to the spectrometer grating model used for all detectors, the more features that are available to fit to, the better.
2) In order for the spectral calibration to apply equally well to all detector arrays, it is highly desirable for the spectral features to be distributed across the focal plane (evenly distributed, ideally).
3) For numerical fitting purposes, it is highly desirable to have the features be sharp (because translational fits are best done at places where radiance varies rapidly with frequency).
4) Most importantly, the calculated positions of the lines must not significantly change spectrally, under any anticipated climatological circumstances.

Table 4.1. Candidate region evaluation for upwelling flux spectral calibration

region #	mod	LM# start	LM# end	array element start	array element end		frequency [1/cm] start	frequency [1/cm] end
1	M1a	. 20	27	21	28	8	2642.94	2635.35
2		34	46	35	47	13	2627.81	2614.97
3		48	56	49	57	9	2612.89	2604.37
4		95	108	96	109	14	2563.85	2550.63
5	M1b	187	200	70	83	14	2355.09	2342.81
6	M2a	256	264	9	17	9	2560.46	2551.53
7		340	356	93	109	17	2469.66	2453.08
8	M2b	461	473	98	110	13	2229.3	2218.02
9	M3	593	617	80	104	25	1397.51	1384.3
10	M4a	709	721	4	16	13	1611.43	1602.64
11		765	781	60	76	17	1571.19	1560.73
12	M4b	820	833	11	24	14	1520.19	1511.67
13		868	893	59	84	26	1489.22	1473.58
14	M4c	944	956	29	41	13	1321.81	1314.7
15		976	984	61	69	9	1303.02	1298.41
16	M4d	1035	1044	26	35	10	1258.74	1253.88
17	M5	1142	1150	27	35	9	1122.45	1118.19
18		1159	1174	44	59	16	1113.44	1105.61
19		1178	1189	63	74	12	1103.53	1097.88
20	M6	1277	1290	3	16	14	1045.11	1039.07
21		1299	1311	25	37	13	1034.94	1029.47
22	M7	1497	1524	56	83	28	952.3	941.94
23		1566	1580	125	139	15	926.26	921.15
24	M8	1648	1661	40	53	14	890.29	885.92
25		1701	1710	93	102	10	872.77	869.87
26	M9	1797	1805	28	36	9	841.4	838.21
27		1828	1840	59	71	13	829.18	824.16
28		1914	1932	145	163	19	797.01	790.58
29	M10	2029	2047	93	111	19	751.02	745.88
30		2066	2090	130	154	25	739.32	731.91
31	M11	2108	2125	5	22	18	727.13	722.04
32		2141	2159	38	56	19	717.31	712.06
33	M12	2258	2278	11	31	21	679.27	674.07
34		2346	2366	99	119	21	657.01	652.16

typical number of detectors per region = 14
minimum= 8

Table 4.1 lists the 34 spectral regions that have been identified as potential candidates for use as upwelling radiance features. A typical spectral region has 14 channels, but the number varies from eight to 26 channels. Regions 30, 31, and 32 are included in Figure 4-3.

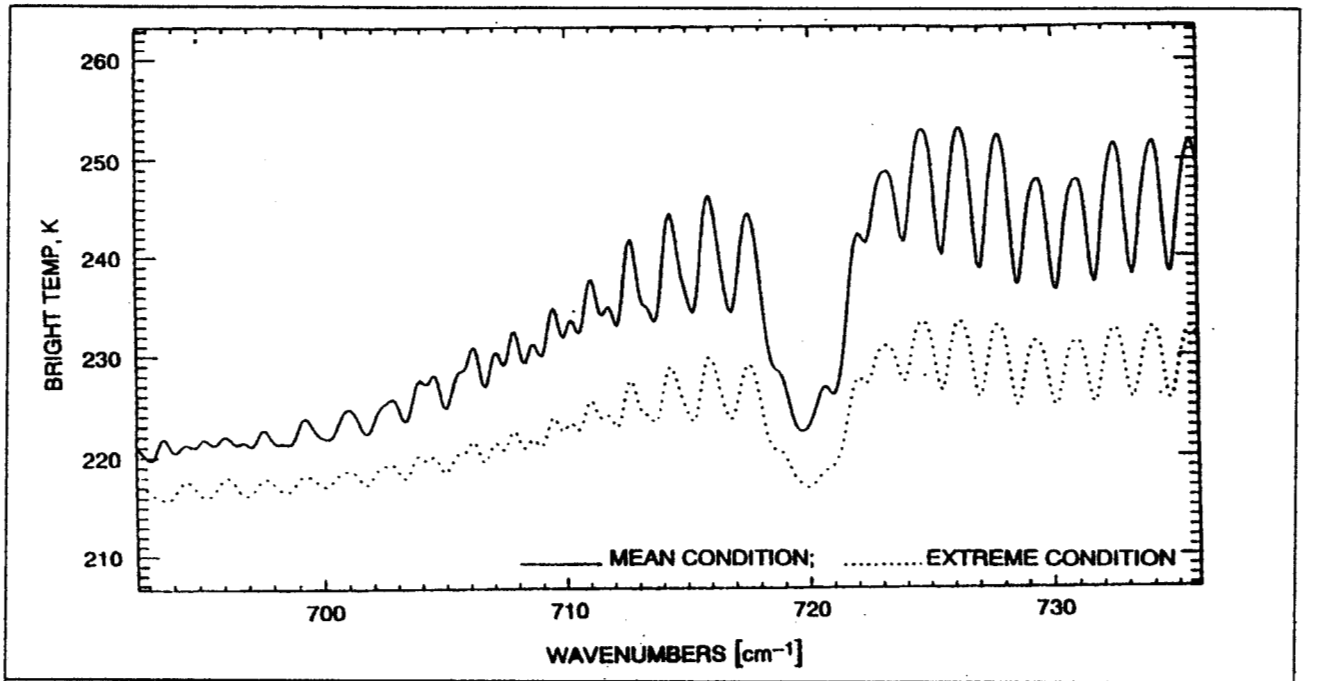

Figure 4.3. The spectrally resolved CO_2 spectral features in the 712 to 736 cm^{-1} region of the spectrum present an excellent region for spectral calibration.

The method used to determine suitability was as follows:

a) The upwelling radiance for a US Standard temperature and moisture profile was calculated using the AIRS SRFs on a frequency grid corresponding to a nominal frequency model, and again for frequency grids corresponding to shifts in X_0 by +/- 5, 10, 15, 20, and 25 microns.

b) Simulated "observed" AIRS spectra were then calculated (for each potential spectral feature) on these 11 frequency grids, for each of eight different extreme climatological conditions. The

eight different climatologies were chosen to simulate anticipated variations in the upwelling radiance spectra.

c) The locations at which the correlations between the "observed" and the pre-calculated spectrum peaked (and the resulting correlation coefficients) were determined, for each spectral feature, for each climatology.

d) Statistics were calculated over the eight climatologies, providing the mean and standard deviation for the observed shifts and correlation coefficients, on a feature-by-feature basis. Table 4-2 shows the results. The suitability flag was determined by requiring the following:

1) A mean shift of less than 1.3 microns (this is equivalent to 1.3% of the SRF FWHM),

2) A standard deviation of the shift of less than 2.6 microns, and

3) A peak correlation coefficient larger than 0.98.

Based on these criteria, 27 of the 35 candidate regions are acceptable. The spectral features were located with a mean error of 0.05 microns. This corresponds to only 0.05% of the SRF FWHM. All arrays except M1b and M4d contain at least one acceptable spectral feature.

Table 4.2. US Standard compared to 8 climatologies (without polar winter) **all region**

region #	mod	shift(um) mean	sigma	1.3	2nd deriv(x1000) mean	sigma	corr.coeff mean	sigma	0.98	2.6	summary good=0
1	M1a	-0.60	1.08	0	0.69	0.01	0.996	0.003	0	0	0
2		1.19	1.04	0	0.18	0.02	0.997	0.003	0	0	0
3		-0.57	0.37	0	0.30	0.01	0.995	0.005	0	0	0
4		-9.41	10.96	1	0.05	0.01	0.993	0.009	0	1	1
5	M1b	-0.73	1.14	0	0.17	0.00	1.000	0.000	0	0	0
6	M2a	-1.30	1.43	0	0.12	0.01	0.999	0.001	0	0	0
7		0.08	2.48	0	0.02	0.00	1.000	0.001	0	0	0
8	M2b	-1.86	2.63	1	0.10	0.00	1.000	0.000	0	1	1
9	M3	-0.02	0.05	0	0.12	0.00	1.000	0.000	0	0	0
10	M4a	-0.21	0.12	0	0.58	0.00	1.000	0.000	0	0	0
11		-0.05	0.26	0	0.25	0.00	0.999	0.001	0	0	0
12	M4b	0.08	0.37	0	0.32	0.00	0.999	0.001	0	0	0
13		0.17	0.17	0	0.15	0.00	1.000	0.000	0	0	0
14	M4c	-0.30	0.99	0	0.26	0.02	0.998	0.004	0	0	0
15		-0.45	0.06	0	0.32	0.00	1.000	0.000	0	0	0
16	M4d	-0.44	6.55	0	0.46	0.08	0.986	0.009	0	1	1
17	M5	-0.90	1.31	0	0.54	0.05	0.988	0.019	0	0	0
18		0.05	1.33	0	0.51	0.02	0.995	0.006	0	0	0
19		-0.07	4.51	0	0.52	0.04	0.993	0.010	0	1	1
20	M6	0.23	0.39	0	0.06	0.00	1.000	0.000	0	0	0
21		1.60	1.84	1	0.52	0.04	0.988	0.019	0	0	1
22	M7	0.91	4.00	0	0.32	0.05	0.980	0.028	0	1	1
23		-1.03	1.28	0	0.35	0.02	0.987	0.013	0	0	0
24	M8	0.13	0.15	0	0.34	0.00	0.995	0.005	0	0	0
25		-0.04	0.13	0	0.31	0.01	0.999	0.001	0	0	0
26	M9	1.17	1.55	0	0.48	0.03	0.997	0.002	0	0	0
27		-0.89	1.56	0	0.52	0.02	0.993	0.008	0	0	0
28		0.60	0.86	0	0.58	0.01	0.976	0.021	1	0	1
29	M10	-0.09	0.31	0	0.55	0.00	1.000	0.000	0	0	0
30		0.04	0.20	0	0.65	0.00	1.000	0.000	0	0	0
31	M11	-0.04	0.34	0	0.55	0.01	0.999	0.001	0	0	0
32		-0.02	1.02	0	0.51	0.00	0.999	0.001	0	0	0
33	M12	0.02	0.25	0	0.42	0.01	0.998	0.001	0	0	0
34		-0.14	1.07	0	0.48	0.01	0.997	0.003	0	0	0

-0.05 microns **27**

all array median position error **total number of good regions**

4.4 Spectral Calibration Error Estimation

The uncertainty in the SRF centroid position determined by the spectral calibration algorithm had four main components:

1. the uncertainty in the spectrometer calibration model (based on pre-launch calibration). The presence of channel spectra in the entrance (order isolation) filters of the AIRS flight model contributes to the basic uncertainty of the accuracy of the spectrometer model.
2. uncertainty in the determination of L_0 and X_0 in orbit based on the finite number of spectral tie-points obtained from the upwelling spectra.
3. the mismatch between the pre-calculated climatology spectra and the actual upwelling radiance.

The magnitudes of the uncertainties differ from array to array. A complete error analysis will be performed based on a full analysis of the final calibration data. We expect that 1% of $\delta\lambda$ requirement will be met.

Accurate knowledge of the SRF FWHM and the SRF wing response is critical for the accurate calculation of the transmittance function in the Radiative Transfer Algorithm (RTA). Errors in the knowledge of the SRF width and/or wing response will mimic spectroscopic errors, which under some conditions may exceed several times the radiometric error. Details of these effects will be discussed in the RTA section of the Level-2 ATBD. Details of the SRF shape, including focus and temperature effects, will be published in the AIRS Spectrometer Calibration Report. Direct determination of the shape of the SRF in orbit is not possible and is not part of the Level-1B calibration algorithm. The indirect validation of the SRF shapes and centroid positions, using upwelling spectral radiances in areas where the state of the atmosphere (temperature and moisture profile) are accurately known, is part of the AIRS Validation Plan. The relevant section of that plan is reproduces in Appendix 7.

5. Spatial Calibration

The AIRS infrared data, with a 1.1 degree effective FOV, will be analyzed simultaneously with microwave data from the AMSU (3.3 degree beam), and the HSB (1.1 degree beam). Knowledge of AIRS FOV location on the ground has to be within a 255 arc second half cone angle. The requirement is easily met by the spacecraft knowledge of the pointing vector within 12.2 arcsec (1 sigma). The selection of several AIRS FOV's within the AMSU FOV is thus based on data from instrument integration. Details of the selection of AIRS FOV clusters located within the AMSU FOV are discussed in the level 2 ATBD. No AIRS infrared pixel interpolation is required or included in the level 1b algorithm.

5.1. Infrared Boresight Validation

The AIRS infrared boresight has relative to the scan mirror axis was verified as part of the ATCF testing. The level 1a software combines the scan mirror encoder data and spacecraft telemetry to determine the infrared boresight. Validation of the AIRS infrared boresight at the team leader facility is planned to facilitate cross-comparisons between AIRS and other instruments on the EOS PM spacecraft. This algorithm is part of the in-orbit validation software, and as such not part of the level 1b software. A description of the concept is included in the following because of general interest.

The algorithm will make use of the statistics of crossings of high contrast scenes (e.g. transitions from land to ocean) to determine a longitude and latitude offset angle between the apparent boundary location and the true boundary location. If the temperature contrast between ocean and land is ΔT_{ol} , the spectrometer noise equivalent temperature per footprint is $NE\Delta T$, the angular footprint diameter is Φ, and the average angle between the cross-track scan and the coastline intersection is α, then the statistical accuracy of the cross-track position accuracy determination from n crossings is

$$\frac{\Delta\Phi(n)}{\Phi} = \frac{NE\Delta T\cos(\alpha)}{\Delta T_{ol}\sqrt{n}} \qquad \text{Eq. 5-1}$$

For typical values of α=45 degree, NEΔT=0.2 K and ΔT_{ol}=10 K, we obtain

Response: This is discussed in Section 3.4. Suitable correction terms will be developed based on the measured response from the LABB stabilized at 205K to 360K in steps of 15K.

3. Concerns about the scan mirror

Question/Concern: The scan mirror non-uniformity is not calibrated. This needs to be investigated thoroughly in vacuum tests before launch. Possible changes in the lifetime of AIRS need to be modeled.

Question/Concern: The ability of the AIRS instrument to monitor differences and changes in the scan mirror emissivity on-orbit for those positions on the mirror used to view the Earth is not established.

Question/Concern: How isotropic is the background radiation so that space, blackbody and earth looks all have the same radiative offset? How will this be tested in vacuum?

Response: This is discussed in the ATBD, section 3.4. The effect is sufficiently small to be neglegible and still meet the AIRS absolute calibration requirements.

Question/Concern: The AIRS scan mirror emissivity may change in orbit due to contamination. Could the scan mirror emissivity be calculated using the cold-space-view experiment proposed by the MODIS and CERES teams. The benefits of a deep space look should be explored.

Response:

1) The AIRS radiometric calibration has no sensitivity to the mean value of the scan mirror emissivity. A scan angle dependent variation in the emissivity would have an effect. This is discussed in Section 3.2.1. Under worst case assumptions the effect is neglegible for AIRS instrument conditions and calibration requirements.
2) It would be desirable to measure the emissivity of the scan mirror at all scan angles for all wavelengths directly in-orbit. Eq.3-13 could then be used to calculate the radiance correction term $\Delta N(\delta)$. However, the proposed experiment does not provide for AIRS the information required to calculate the emissivity as function of scan angle.

It has been proposed to do a cold-space scan maneuver with the Aqua satellite to measure radiometric parameters, including scan mirror properties, for CERES and MODIS. In this experiment the spacecraft nadir position is rotated 180 degrees and the scan mirror steps from -49 to +49 degrees to scan cold space. The experiment takes about 30 minutes. Using the notation of section 3 the experiment provides 90 equations for the unknown 96 values of the emissivity

$$(V(\delta)z-V(s)) / G = Ns * (e(\delta)-e(s)),$$

This system of equations can only be solved with somewhat arbitrary assumption. Equation for e(s) and e(b), related to knowledge of the transmission of the scan mirror in cold space view and OBC view position, are not available from this experiment. If we assume an average responsivity R, we can solve for the 90 values of (e(δ)-e(s)). We can then calculate a standard deviation of the emissivity relative to the mean

Δe=STDEV(e(δ)-e(s)),

and use it to update the estimated error incurred from neglecting the scan mirror emissivity in the calibration equation.

4. Concerns about the spectral calibration

Question/Concern: How does the grating constant vary with temperature? Can the required thermal stability be achieved?

Response: Level 1b ATBD IR spectrometer, section 2.1.

The effect of spectrometer temperature on the spectral calibration was measured in TVAC. A spectrometer temperature change causes an apparent shift in the focal plane position of 2.7 micron/degree K. Since the SRF width is equivalent to 100 microns, this corresponds to a shift of 2.7% of the SRF width per degree K temperature change. The effect is due to the expansion coefficient of the Aluminum.

The spectral stability achieved under simulated orbital conditions exceeds the requirement by a factor of 10. During the simulation of 24 hours in orbit the observed amplitude of the

apparent focal plane motion was +/- 0.3 microns. A shift of less than 0.5 micron, corresponding to 0.5% of the SRF width, is practically neglegible.

The temperature of the spectrometer has a time constant of 20 hours and the temperature is actively regulated to within 0.01K. After thermal equilibrium is achieved (estimated to take about two week, based on the experience in the ATCF), the spectral calibration of AIRS is expected to be extremely stable. The activities planned under routine spectral calibration are thus more in the nature of spectral stability calibration monitoring.

Software has been developed for the level 2 processing to track spectral calibration shifts of less than 5% of the SRF width from the nominal frequencies using regression based interpolation. With the observed stability the tracking software will not be necessary.

Question/Concern: There needs to be an estimate of the error due to [the] use of calculated radiances (which are imperfect) for spectral calibration. How do thin cirrus affect clear scene spectral calibration?

Question/Concern: AIRS's approach to cloud detection may be inadequate for certain hard to detect cloud types and may affect the on-orbit spectral calibration.

Response: Level 1b from ATBD IR spectrometer, section 4.1. and Table 4.2.

Since the correlation algorithm is invariant to additive and multiplicative terms in the radiances, the upwelling spectra need not be known very accurately, as long as the spectral features due not shift. Spectral features due to resolved isolated lines do not shift, but some spectral features which are only partially resolved show an apparent shift. Spectral features which show excessive sensitivity have been identified in Table 4.2. and have been rejected.

1. Clouds will have little effect on the spectral calibration, since they do not have a significant spectral signature over the narrow spectral range used in the frequency calibration.
2. Only clear fields of view will be used for spectral calibration. Clouds will be detected as part of the cloud-clearing algorithm. Fields with thin cirrus clouds will be identified by their broad spectral signature in the 11 micron area.
3. The spectral calibration algorithm rejects data if the correlation coefficient peak is less than a predefined threshold unique to each spectral region.

Question/Concern: AIRS proposes to monitor spectral calibration using Earth scene radiances rather than a well-characterized, calibration source.

Response: See Table 4.2. For the AIRS accuracy requirement the upwelling spectral radiance is the one obvious and only reliable spectral calibration source.

5. Concerns about Level 1b Validation

Question/Concern: The position of the AIRS instrument team on the usefulness of vicarious calibration for the on-orbit validation of instrument calibration is not presented in the ATBD and it is a bit confusing.

Response:

The AIRS team has the goal of using vicarious validation for routine processing, i.e. ground-truth using sea-surface floating buoys will be used in the initial validation process and as part of the routine level 1b QA effort. This monitoring effort includes scatter diagrams of the deviations (residuals) of the observed temperature from the ground-truth temperature

1) as function of temperature (270K to about 310K) and
2) as function of scan angle.

The process of vicarious validation differs from the process of vicarious calibration: Vicarious validation minimizes the residuals between measured radiances and radiances calculated based on ground-truth data by analyzing the root of the discrepancy and fixing the "error" at the root. This not only eliminates a bias under a specific condition, e.g. at 270K surface temperature, but it decreases the bias at other conditions, e.g. much colder temperatures which can not be readily validated via ground truth. If spectral patterns in the residuals suggests a problem with the level 1b software, appropriate corrections will be made in the software. This procedure eliminates bias and decreases the residual scatter. Vicarious calibration by empirically minimizing residuals between calculated and observed only eliminates a bias at a specific condition (perhaps only at a validation site). The section on AIRS level 1b validation from the AIRS Validation Plan, expected be released on 15 December 1999, is reproduced for information as Appendix 7 of the level 1b ATBD.

Appendix 2. Dictionary of Abbreviations

ADC	Analog to Digital converter
AIRS	Atmospheric Infrared Sounder
AMSU	Advanced Microwave Sounding Unit
ATBD	Algorithm Theoretical Basis Document
ATCF	AIRS Test and Calibration Facility (TVAC)
CSV	Cold Space View
DCR	DC Restore (of the electronics)
DN	Data Number
DOD	Department of Defense
EM	Engineering Model
EOS	Earth Observing System
FOV	Field of View (projected on the ground pertaining to one dwell time)
FM	Flight Model
FRD	Functional Requirements Document
GSFC	Goddard Space Flight Center
HgCdTe	Mercury-Cadmium Telluride
HIRS	High Resolution Infrared Sounder
HSB	Humidity Sounder Brazil
IFOV	Instantaneous Field of View. Smaller or equal to the FOV.
IR	Infrared

ITS	Interagency Temperature Sounder
JPL	Jet Propulsion Laboratory
MODIS	Moderate Resolution Imaging System (on EOS-Am and PM)
MSU	Microwave Sounding Unit
NASA	National Aeronautics and Space Administration
NEDT	Noise Equivalent Delta Temperature
NEN	Noise Equivalent Radiance
NIR	Near Infrared (between 1 and 3 microns)
NIST	National Institute of Standards
NOAA	National Oceanic and Atmospheric Administration
NWS	National Weather Service
OBC	On-Board Blackbody Calibrator
OBS	On-Board Spectral reference source
PC	Photoconductive Detector
PFM	Proto Flight Model
PRT	Platinum Resistance Thermometer
PV	Photo Voltaic Detector
QA	Data Quality Assessment
SRF	Spectral Response Function
TBD	To Be Determined
TVAC	Thermal Vacuum Chamber
VIS	Visible wavelength

Appendix 3. Radiometric calibration coefficients and preliminary results.

1. The radiometric calibration coefficients were evaluated using the LABB. The LABB is a wedge cavity design, larger, but otherwise similar in its basic to the OBC, but with selectable temperature between 190K and 360K. It is located at a distance of 11.5" from the scan mirror. The walls are coated with Aerogalze Z-302, which has a reflectivity of less than 0.11. For the wedge angle of 27.25 degrees and the AIRS geometry more than 6 specular reflections are required before the beam exits the cavity. The LABB emissivity is theoretically is better than $(1-(0.11)^6)$, i.e. better than 0.9999. The LABB output is given directly by the Planck function. The Platinum Resistance Thermometers (PRT) were NIST calibrated. For the OBC calibration test the LABB set to ten temperatures, T.labb, between 205K and 340K. Using the terms defined in section 3, we have ten equations in 4 unknows

$$\text{Planck}(T.k) = a.1 * W + a.2 * W^2 + a.3 * W^3 + a.4 * W^4$$

and solve for a.1, a.2, a.3 and a.4 in a least squares sense.

Figure A.3.1. shows results of preliminary calibration data analysis. If we write

$$N = a.1 * W + a.2 * W^2 + a.3 * W^3 + a.4 * W^4$$

$$= a.1 * W (1 + a.2 * W / a.1 + a.3 * W^2/a.1 + a.4 * W^3/a.1)$$

where W is the signal in data numbers from a 250K blackbody, then $a.2 * W / a.1$ is a measure of "Nonlinearity". This measure is plotted in Figure A.3.1.

Coefficients based on the final calibration of the AIRS PFM have not been generated.

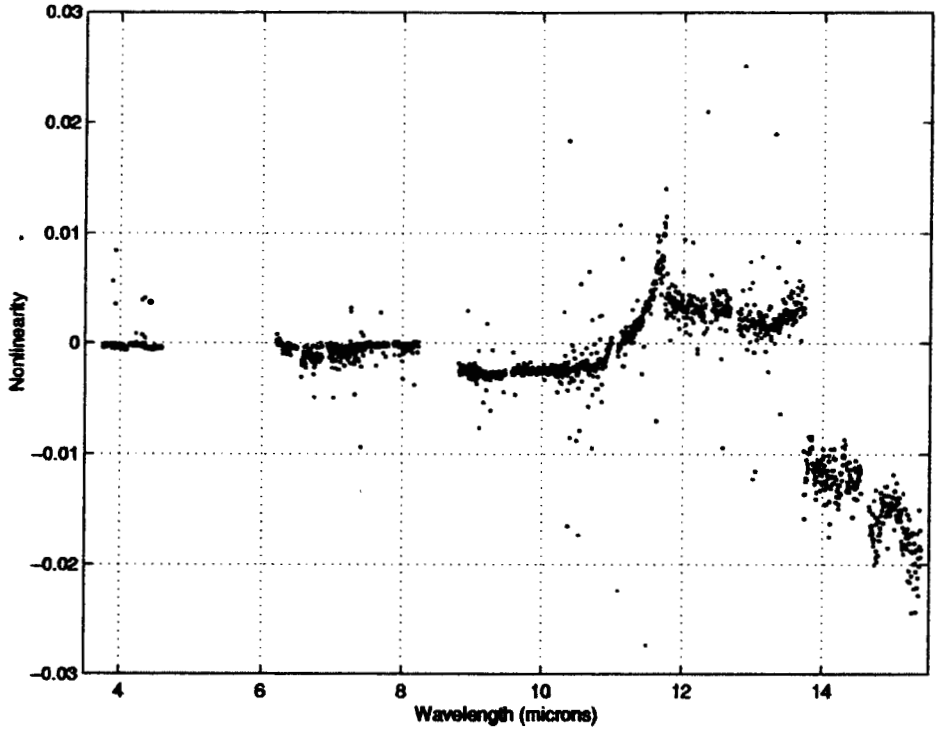

Figure A.3.1. shows the effect of non-linearity at 250K. The effect is extremely small for the PV detectors (short of 11 microns). For the PC detectors at the longest wavelengths the correction is about 2%.

2. OBC calibration:

The OBC was calibrated pre-flight relative to a Large Area Black Body (LABB), a NIST traceable secondary standard developed by BOMEM, Inc., of Quebec City, Canada. For the OBC calibration the LABB was set to 310K. Using the definitions of section 3.

$$N.obc = a.1 * W.obc + a.2 * W.obc^2 + a.3 * W.obc^3 + a.4 * W.obc^4$$

Since the OBC was accurately temperature regulated at T=308.0K, we can define an effective emissivity

$$e(nu) = N.obc(nu)/Planck(308,nu).$$

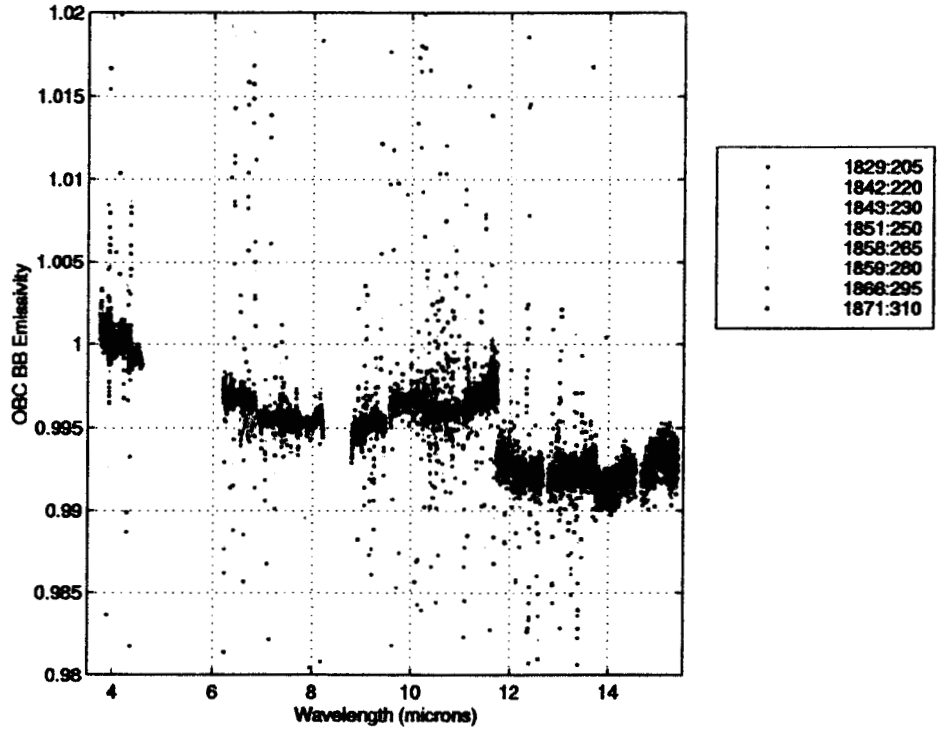

Figure A.3.2. Apparent emissivity of the OBC for all detectors. The OBC Temperature Sensor weighted reading was 307.9K ±0.1K.

The emissivity of the OBC, shown in Figure A.3.2 based preliminary data analysis, is within 1% of unity. This is qualitatively very encouraging, since the predicted OBC emissivity is 0.999. A small temperature gradient (about 0.2K) across the OBC causes the apparent emissivity to be slightly wavelength dependent.

Use of the OBC for the radiometric calibration equation requires the definition of a nominal brightness temperature which ties the LABB based radioemtric calibration, T_obs, into the output of the OBC temperature sensors in the telemetry, Tobc.sens.

Define

Tobc.sens = a * T1 + b * T2+c * T3 +d * T4 and

T.obc = Tobc.sens + DT.obc

The mean OBC temperature calculated over all frequencies is 308.22K. This is in very good agreement with the OBC thermostat setpoint of 308.0K. However, based on the design and the location of the temperature sensors in the OBC we would expect a=b=0.45, c=0.09 and d=0.01. With these coefficient we found throughout the testing Tobc.sens = 307.92K, resulting in DT.obc = 0.30 K. A re-evaluation of the OBC temperature sensor calibration is in process.

If the temperature of the OBC should change in orbit, then DT.obc defines the relationship between the reported temperature and the temperature to be used in the calibration equation.

Appendix 4. Polarization Correction term

1. Instrument polarization

Figure A.4.1. shows the modeled average transmissions of the AIRS spectrometer and scan mirror modified by the measured polarization. Although correction equation E. 3-3 only requires the polarization, observation of the S and P components has allowed us to attribute the bulk of the spectrometer polarization to the grating.

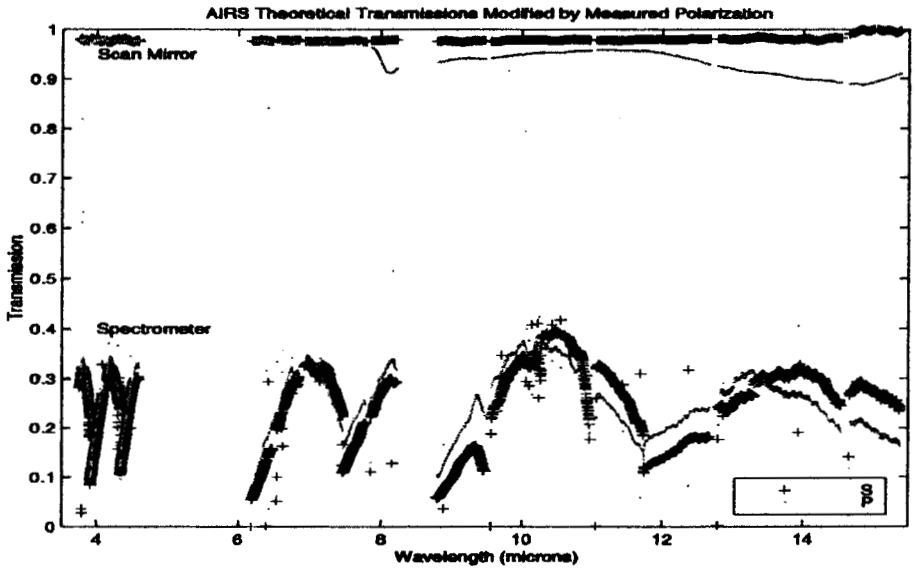

Figure A.4.1. Spectrometer polarization and scan mirror polarization are used to determine the scan angle dependent radiometric correction term.

Extensive modeling of the components that contribute to the polarization have yielded good correlation between prediction and measurement giving good confidence in our polarization estimates (Ref. 8). Spectrometer polarization was derived from system level polarization measurements and dividing out the measured polarization of the scan mirror. Scan mirror polarization was measured for the AIRS scan mirror witness samples by MIT Lincoln Labs (Ref.9).

2. Measured Scan Angle Dependent Radiometric Correction Term

Measurements were obtained on the AIRS system in its final flight configuration (November 1999) to verify the validity of the algorithm used for the scan angle dependent correction term. Based on preliminary analysis the data show excellent agreement between the predicted correction terms and the radiances.

The AIRS instrument was allowed to view the Large Area Blackbody (LABB) at scan angles from about –48° to +36°. The radiometric offset due to polarization , $dN_{p,meas,}$ was calculated as the difference between the radiance as derived using the internal OBC, and the known radiance of the LABB,

$$dN_{p,meas} = N_{calc} - N_{calc,nadir}$$

The derived (calculated) radiance for the LABB from the AIRS measured digital number was obtained using the measured dn's and averaging over all scans:

$$N_{calc} = N_{OBC} \bullet \frac{\frac{1}{Nscans} \sum_{i=1:Nscans} (dn_{LABB,i} - dn_{SPACE,i})}{\frac{1}{Nscans} \sum_{i=1:Nscans} (dn_{OBC,i} - dn_{SPACE,i})}$$

where

N_{calc} = *Derived radiance of theLABB (W/m^2-sr-μm)*

dn_{LABB} = *Signal measured while viewing the LABB*

dn_{SPACE} = *Signal measured while viewing the space*

The fractional radiometric correction and temperature correction were then calculated from the radiometric offset.

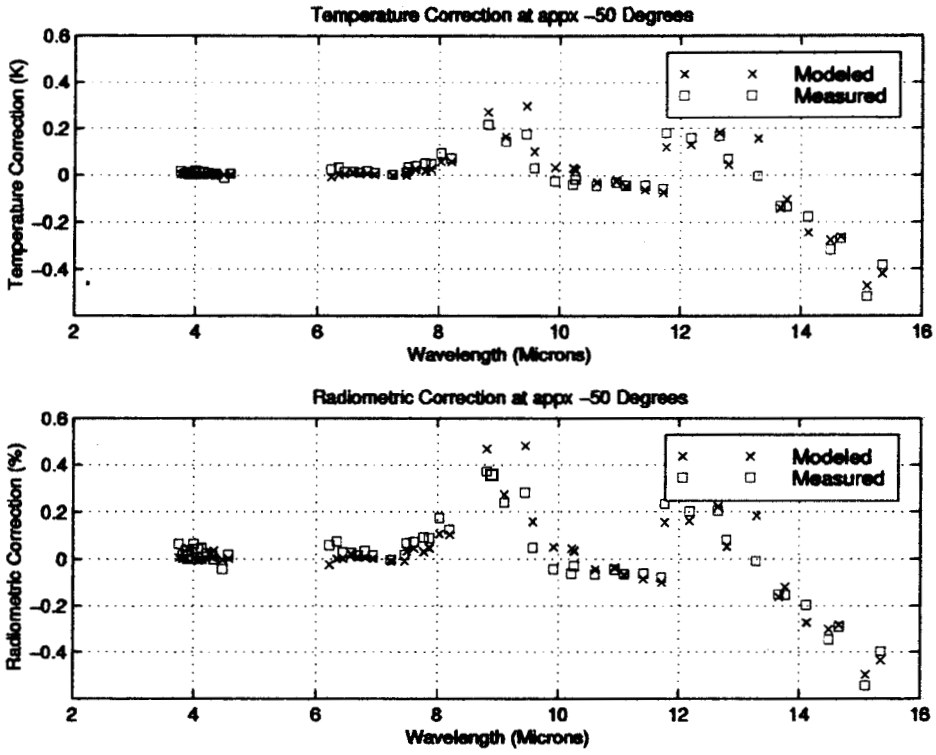

Figure A.4.2. Radiometric offset at –50 degrees (compared to nadir) for the 51 reference detectors. Residual errors from the model and measurements are mostly less than 0.1K with a few exceptions on the order of 0.2K.

We performed the analysis on the 51 reference detectors (three per array, one at the center and one on each end of the 17 IR modules) at –50 degrees. The results are shown in Figure 3.3. The difference between the expected correction (model = x) and the measured offset is less than 0.05K at wavelengths shorter than 8.5 microns. At longer wavelengths there is excellent correlation between measurements and model. The differences are typically less than 0.1K, but there are two cases of 0.2K difference. The cause of this is currently under investigation.

Appendix 5. Temperature change which corresponds to a 1% change in radiance

Table A.5.1. Temperature change which corresponds to a 1% change in radiance.

Temperature change equivalent for a flux increase of 1 %

array name	mean array microns	Scene Temperature [degree K] 205	220	235	250	265	280	295	310	325
M1a	3.8267	0.11	0.13	0.15	0.17	0.19	0.21	0.23	0.25	0.28
M2a	4.2196	0.12	0.14	0.16	0.18	0.21	0.23	0.25	0.28	0.31
M1b	4.0125	0.12	0.13	0.15	0.17	0.20	0.22	0.24	0.27	0.29
M2b	4.4678	0.13	0.15	0.17	0.19	0.22	0.24	0.27	0.30	0.33
M4a	7.2063	0.21	0.24	0.28	0.31	0.35	0.39	0.43	0.48	0.53
M4b	6.3469	0.18	0.21	0.24	0.27	0.31	0.34	0.38	0.42	0.46
M3	6.7002	0.19	0.22	0.26	0.29	0.33	0.36	0.40	0.45	0.49
M4c	7.6333	0.22	0.26	0.29	0.33	0.37	0.41	0.46	0.51	0.56
M4d	8.0403	0.23	0.27	0.31	0.35	0.39	0.44	0.48	0.53	0.59
M5	9.1435	0.27	0.31	0.35	0.40	0.44	0.49	0.55	0.61	0.66
M6	9.9200	0.29	0.33	0.38	0.43	0.48	0.54	0.59	0.65	0.72
M7	10.6300	0.31	0.36	0.41	0.46	0.51	0.57	0.63	0.70	0.77
M8	11.4108	0.33	0.38	0.43	0.49	0.55	0.61	0.68	0.75	0.82
M9	12.2141	0.35	0.41	0.46	0.52	0.59	0.65	0.72	0.80	0.87
M10	13.2723	0.38	0.44	0.50	0.57	0.64	0.71	0.78	0.86	0.94
M11	14.1455	0.41	0.47	0.53	0.60	0.67	0.75	0.83	0.91	0.99
M12	15.0336	0.43	0.50	0.57	0.64	0.71	0.79	0.87	0.96	1.04

Appendix 6. Channel Spectra

An interference transmission filter , deposited on a substrate of physical thickness t and refractive index n, made with accurately parallel surfaces acts like a Fabry-Perot plate: The transmission is modulated with repeat frequency $\delta\nu = 1/(2*n*t)$. This effect is called channel spectrum. The amplitude of the channel spectrum roughly proportional to the reflectivity of the surface. For a real transmission filter the reflectivity inside the passband is very small, but not zero. The channel spectrum can be eliminated by designing the filter with a small wedge angle, about 3 arminutes, such that the front and back surfaces of the filter are no longer parallel. Due to a design oversight the 1 mm thick Germanium substrates of the order isolation filters at the spectrometer entrance slit were designed with insufficient wedge angle. As a result the transmission spectra at the entrance slit filters contain channels spectra. With t=0.1 cm and n=4 we get a repeat frequency of $\delta\nu$=1.2 cm^{-1} . This channel spectrum is clearly visible in the transmission spectrum of a typical entrance filter (array M3) shown in Figure A.6.1.

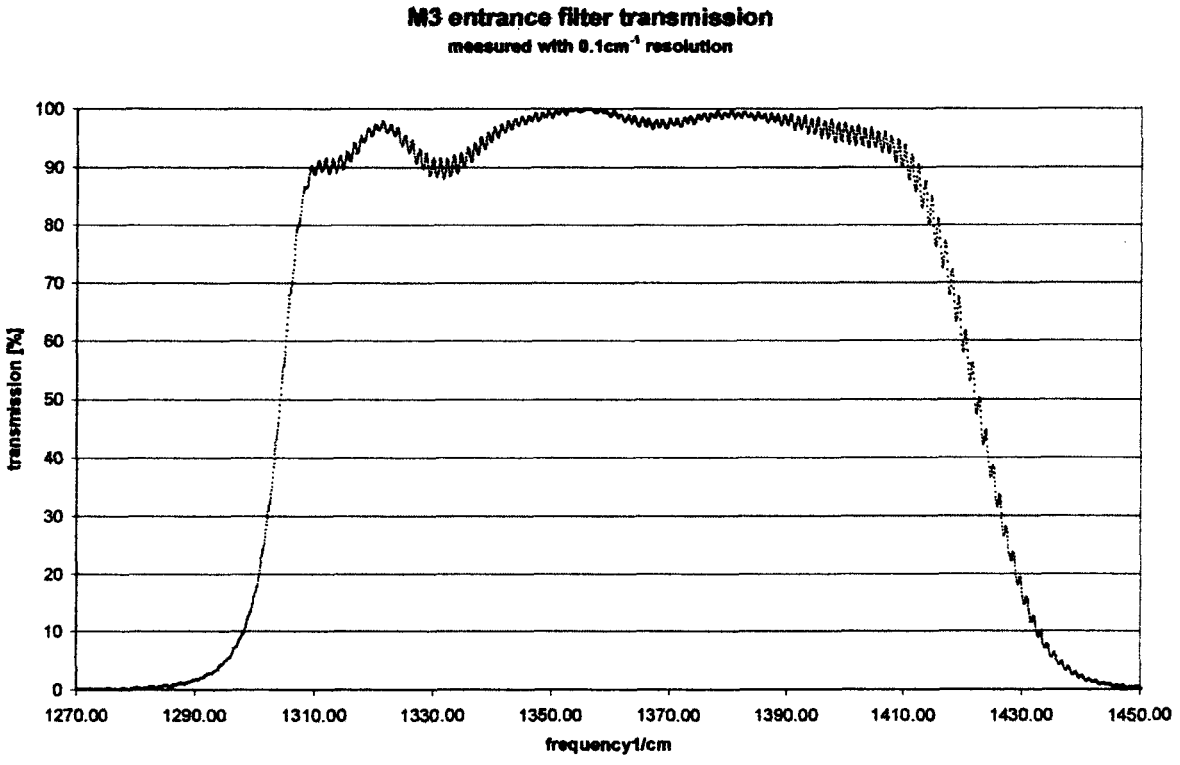

Figure A.6.1. AIRS Entrance filter for Array M3 with channel spectra

The channel spectrum peak-to-peak amplitude is about 3%. The channel spectrum effects the fine details of the SRF shape. This is illustrated in Figure A.6.2. The figure shows the SRF at 1399.9 cm^{-1} which would be observed in the absence of the channel spectrum (solid dots) and in the presence of channel spectra (open triangles). For the

select channel the shift of the SRF peak by about 2% of the SRF width is clearly visible. The shift depends on the relative position of the channel spectrum peaks and the SRF position, and varies from zero to +/- 2% peak. This effect clearly visible in the raw spectral calibration data, e.g. Figure 4.3. Since the spectrometer is temperature controlled to an accuracy of 0.01K, the effect of the channel spectrum is frozen into each SRF.

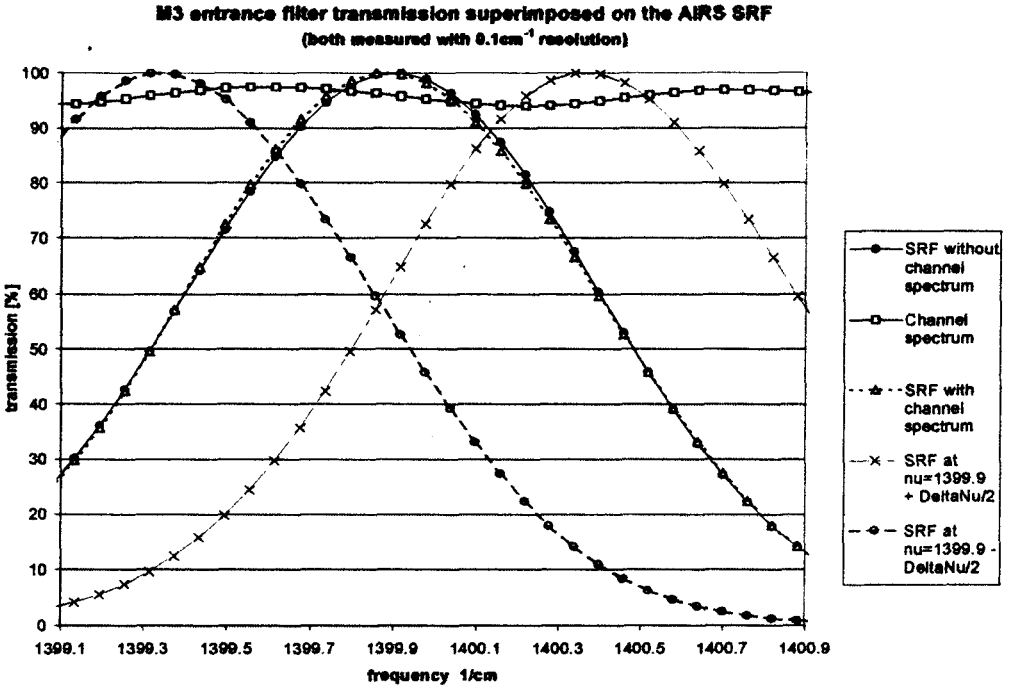

Figure A.4.2. Three typical SRF response functions with the effect of channel spectra superimposed on the SRF in the center. The effect is small, but will be eliminated as part of the in-orbit calibration.

The small change in the SRF due to the presence of channel spectra has no effect on the level 1b algorithms, since the calibration sources have no spectral features at the spectral width of the channel spectra. However, the upwelling spectra contain spectrally sharp absorption and emission features. Neglecting the channel spectra in the forward algorithm, i.e. in the calculation of the upwelling spectral radiance, can in some spectral regions result in errors as large as 0.5K in the calculated brightness temperature. Typical errors are much smaller. This effect will be minimized by

1) the determination of the location of the channel spectrum relative to the SRF's as part of the in-orbit activation and calibration. The exact shape of the SRF used in the forward algorithm will then explicitly include the channel spectrum effect.
2) carrying the residual effect of the channel spectrum as one term in the overall uncertainty estimate of brightness temperature calculated by the forward algorithm. This is discussed in the level 2 ATBD.

Appendix 7. Validation of Level 1B Spectral Radiances by L. Larrabee Strow, UMBC

1 Background

This section addresses the validation of the AIRS Level1B calibrated radiances, with an emphasis on their spectral nature. The radiometric and spectral calibration of AIRS is discussed in some detail in the AIRS Instrument Calibration Plan and in the AIRS Level 1b ATBD. The term spectral calibration refers to our knowledge of the AIRS spectral response functions (SRFs), which includes their shape, spectral location (centroids), and how these quantities change with temperature and AIRS focus.

Validation of the AIRS Level 1B radiances involves not only validation of the radiometric accuracy of these radiances, but also validation of the SRFs that gives AIRS its high spectral resolution. AIRS Level 2 retrievals use a fast radiative transfer model (AIRS-RTA) to minimize the differences between the observed and computed radiances. Since the forward model is very sensitive to the exact form of the AIRS SRFs, we consider the validation of the SRFs part of Level 1B validation. Although extensive ground calibration of AIRS has given us much information on the form of the SRFs, they cannot be known exactly until AIRS is in orbit for reasons described later. (See the AIRS Level 1 ATBD for details on in-onbit spectral calibration).

The validation of the AIRS spectral calibration will rely on comparisons between observed and computed radiances, so it will also involve simultaneous validation of the forward model spectroscopy and the fast radiative transfer parameterization. Separately validating the various aspects of the Level 1B radiances (*i.e.*, radiometric calibration, SRF knowledge, spectroscopy, fast model parameterization) will require a wide range of inter-comparisons under many atmospheric conditions. Although it may appear difficult to separate out these various effects, the copious redundancy (in terms of weighting functions) in the AIRS spectral channels, coupled with good models for instrument errors and spectroscopic errors, should allow us to de-couple these effects and separately validate them in large part.

Validation of the AIRS radiometric calibration is partially addressed here, but is also covered in the validation of sea-surface temperature products. AIRS sea-surface radiances provide the best opportunity for validation of the components of the AIRS absolute radiometric calibration that are common to all detectors, such as the temperature/emissivity of the on-board blackbody calibrator (OBC) and scan mirror angle effects. The spectral validation activities discussed in this section will depend in-part on validation of the absolute radiance calibration (at least for high radiance scenes) via observations of well characterized surface sites such as the sea-surface.

Conceptually, AIRS convolves the Earth's up-welling monochromatic radiances with the AIRS SRFs. The earth view detector counts are converted into radiances in the standard way using

detector space view counts and on-board blackbody calibrator (OBC) view counts recorded in-between each scan line. These measurements, combined with the OBC temperature, provide the basic radiometric calibration of AIRS. Early ground calibration results generally suggest that the OBC illumination of the detector focal plane is quite uniform, that the detector responses are very nearly linear, and that scan angle effects are relatively small. Consequently, we hope that absolute radiometric calibration and validation will primarily be involved with characterizing the OBC temperature and stability, which are essentially independent of spectral channel.

The overall goal is to validate and possibly improve our *models* of the AIRS instrument behavior, the AIRS-RTA, and the spectroscopy in the AIRS-RTA and in doing so validate the AIRS Level 1B radiances. Since these models are largely independent of scan angle and cloud amount, this process will concentrate on nadir views of fields deemed very clear. Figure 1 illustrates the basic flow of information in the Level 1B validation, highlighting the comparison of computed and observed radiances in the ``Radiance Residual Analysis" box.

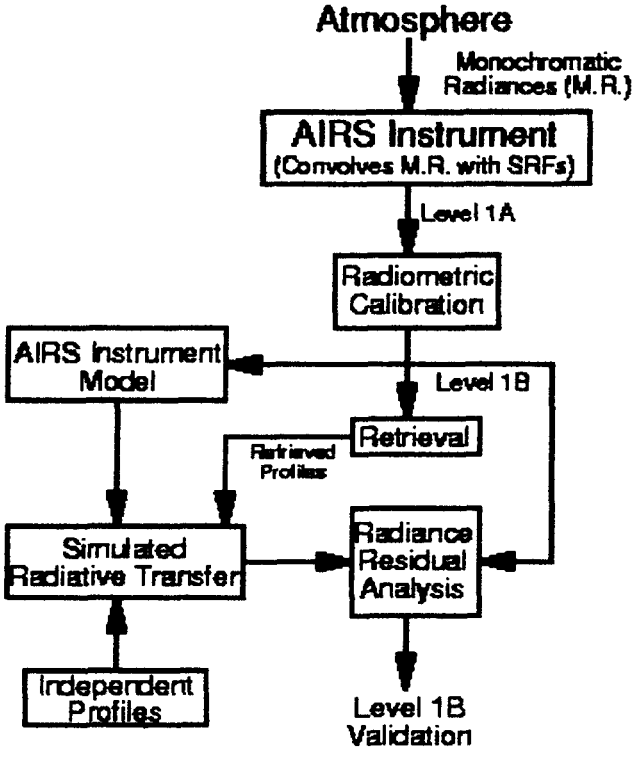

Figure 1: Top level diagram of the AIRS Level 1B validation process.

2 AIRS Instrument Spectral Model

AIRS has 2378 spectral channels that reside on 17 different linear detector arrays. Each detector serves as an exit slit for the AIRS grating spectrometer. AIRS uses 11 entrance slit apertures, which means that some arrays use the same entrance slit. The 2104 channels above 729 cm^{-1}, which are photo-voltaic (PV) detectors, consist of redundant pairs, giving a total of ~ 4500 channels. The detectors below 729 cm^{-1} are photo-conductive detectors with no redundancy.

The AIRS instrument spectral model has three basic components, the grating model, the SRF shape, and the entrance filter fringe positions, which combined together are used to simulate AIRS radiances and to build the fast model (AIRS-RTA).

Grating Model: As discussed in the AIRS level 1b ATBD, a relatively simple model based on the standard grating equation is able to model the AIRS wavenumber scale, at least on a per array basis. This model gives us the ability to predict the SRF centroids for each detector within an array given knowledge of the centroid of at least one detector on that array. The dependence of the grating model on both the instrument temperature, and focus, will be determined from ground calibration data. Once in orbit, up-welling radiances will be used to determine the absolute wavenumber positions of a sub-set of detectors. This information, combined with the grating model, will then allow us to determine the centers of every AIRS detector. Several arrays do not sense sharp, profile independent, features in the up-welling radiances, so we will have to use the grating model to transfer absolute calibration from one array to another. Since the focal plane is a rigid entity, this transfer should be highly accurate.

SRF Shape: The shape of the AIRS SRF is determined by a combination of the grating resolution, dispersion, size of the entrance slit apertures and the detector widths, and instrument scattering (important for the low-level SRF response). Extensive ground calibration tests enabled reasonably accurate measurements of the shape of all ~ 4500 channels, with some signal-to-noise limitations for the long-wave arrays. A simple analytic model has been developed that appears to have sufficient accuracy to model all the grating spectrometer SRFs with just a few parameters per array. In addition, the change in the SRF width with de-focus has been measured during ground calibration. In the improbable case that AIRS suffers any significant de-focus during launch, the SRF widths can be estimated from the absolute wavenumber calibration via the grating model we have developed. It will be very difficult to calibrate the grating spectrometer SRF shape (SRF width, wings) in orbit. We can only determine if the AIRS radiances are consistent with our estimate of their in-orbit shape.

Fringes: The actual total SRF shape of AIRS has another component due to the existence of channel spectra (fringes) in the entrance slit aperture filters. Most of these 11 filters have some

spectral regions containing interference fringes. These fringes have a nominal spacing (free spectral range) of 1.2 cm^{-1}, and a contrast of up to ±5% max. The fringe spacing is small enough to potentially impact all of the AIRS SRFs, which are in practice the entrance aperture transmittances times the ``pure" grating spectrometer SRFs. The positions of the peaks of the entrance aperture fringes are sensitive to temperature via the index of refraction of the filter's germanium substrate. The fringe peaks shift the equivalent of -9.96 microns/degK, while the SRF centroids shift –2.7 microns/degK. Since the width of the SRF is 100 microns (in focal plane coordinates), a change of 0.1degK in spectrometer temperature corresponds to a shift of the fringe peaks of 1% of the SRF. Consequently, the fringes will effectively be frozen relative to the SRFs once the AIRS has temperature stabilized in orbit to within 0.1K of the setpoint of the spectrometer thermostat. The fringe positions relative to the SRF centroids can be inferred in orbit from the temperature dependence of the detector gains. (Basically, the detector gains see the modulation of the overall spectrometer transmission as the fringe peaks shift in wavenumber as the filter (and spectrometer) temperature is changed using the thermostat.) Detailed validation of the Level 1B radiances will therefore involve independent tests to determine if the in-orbit calibration of the fringe peak positions is sufficiently accurate.

3 Spectroscopy, kCARTA, AIRS-RTA

Comparisons of observed and computed AIRS Level 1B radiances depends on the accuracy of the AIRS spectral calibration and on the accuracy of the spectroscopy used in the computation of the simulated radiances. The accuracy requirements for the AIRS radiative transfer model are demanding, and will require the best available spectroscopy and line-by-line codes. In addition, the speed requirements for the Level 2 retrievals requires the use of a fast radiative transfer model (which we call the AIRS-RTA) that is based on parameterizations of atmospheric transmittances suitably convolved with the AIRS SRFs. This parameterization is discussed in some detail in the Level 2 AIRS ATBD.

The spectroscopy used in the AIRS-RTA is derived from kCARTA (kCompressed Atmospheric Radiative Transfer Algorithm), which is a monochromatic radiative transfer code based on compressed look-up tables of atmospheric transmittances. These look-up tables are created using a very accurate, but slow, line-by-line code developed at the University of Maryland Baltimore County, called UMBC-LBL. UMBC-LBL is a state-of-the-art line-by-line algorithm that includes features not found in other line-by-line codes such as P/R branch line-mixing in CO_2.

kCARTA will be used as the AIRS reference radiative transfer algorithm. kCARTA's primary purpose is for the generation and validation of the AIRS-RTA. However, it will also be useful for (1) early validation of the AIRS Level 1B radiances before the AIRS channel center frequencies have stabilized, (2) testing effects of new spectroscopy on AIRS simulated radiances for possible

inclusion in the AIRS-RTA, and (3) providing AIRS radiances convolved with trial SRF models that are needed for Level 1B validation.

We independently validate the line-by-line algorithms by comparisons with new, better laboratory data when available. kCARTA is validated by comparisons to other line-by-line codes (GENLN2, LBLRTM) and by using it to compute validated radiances measured by the HIS/NAST-I instruments that fly on NASA's ER-2.

The AIRS-RTA is validated before launch by comparing radiances it produces to those computed with kCARTA, using an idependent set of profiles (profiles other than those used to perform the regressions for the fast model parameters). The AIRS-RTA is dependent on a proper statistical selection of profiles used in the transmittance regressions (see the AIRS Level 2 ATBD for details). If comparisons of radiances computed with the AIRS-RTA disagree with kCARTA computed radiances when using profiles from actual AIRS retrievals, then our regression profile set must be re-examined. Because both the atmospheric spectroscopy and the AIRS instrument model (SRFs) are fixed in the AIRS-RTA, it cannot be used for some validation activities.

4 Validation Approach

The basic approach to Level 1B validation is to use independent estimates of the atmospheric state to compute simulated AIRS observed radiances, and compare these with the observed radiances. Our overall goal is to improve the instrument, radiative transfer, and spectroscopic *models* in reasonable, understandable ways in order to reduce the radiance residuals. Since these models are largely independent of scan angle and cloud amount, this process will concentrate on nadir views of fields deemed very clear.

There is a high level of redundancy in the AIRS channels in the sense that many channels have very similar forward model weighting functions. The retrieval algorithms only use several hundred AIRS spectral channels, generally those with narrow weighting functions in regions where a single gas dominates the radiance. This leaves many channels with somewhat wider weighting functions that probe the same part of the atmosphere as a combination of channels used in the retrieval.

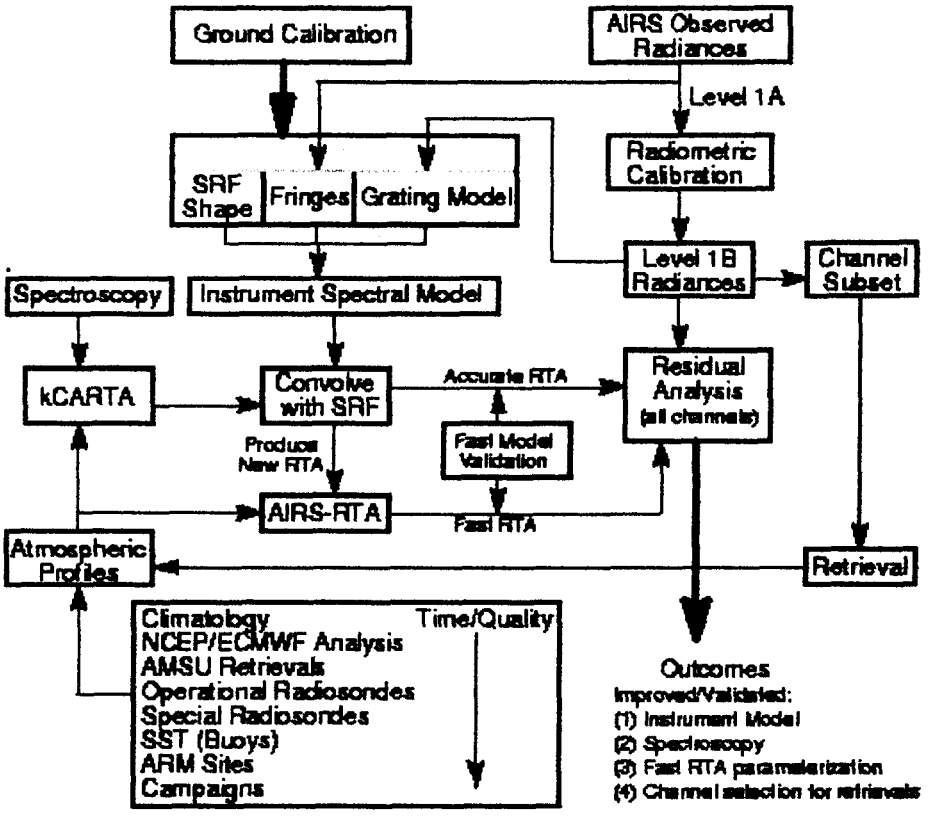

Figure 2: Detailed flow of Level 1B validation activities.

Instrument errors, and to some extent spectroscopic uncertainties, will not be strongly correlated with a channel's weighting function. Given an independent assessment of the observed atmospheric profile, examination of the wavenumber dependence of the observed minus calculated radiances (the residuals) should allow us to detect patterns that correspond to different error sources. Analysis of these residuals will have to take into account our understanding of the errors associated with (1) the independently measured atmospheric profiles, (2) expected patterns in the uncertainty of the spectroscopy, (3) expected error patterns in the (AIRS-RTA) parameterization, (4) behavior of the instrument model if inadequately characterized, and (5) uncertainties (and global variations) of atmospheric gases, such as CO_2, CH_4, and N_2O.

This process will start very early in the deployment of AIRS by comparing observed radiances with radiances computed using climatology. This type of validation will only detect rather severe instrument errors and glaring software bugs. As time progresses we will use ever better independent estimates of the atmospheric state as input to our computed radiances for comparison with the AIRS observed radiances. This includes profiles from (1) the NCEP or ECMWF analysis, (2) AMSU retrievals once they are available, (3) operational radiosondes, (3) special radiosondes launched during the time of AIRS overpasses, (4) ARM site data, and finally (5) intensive in-situ

campaign data. As the quality and amount of in-situ profile data improves, our validation analysis will also become more statistical in nature. For example, validation of radiances sensitive to lower tropospheric water vapor are problematic on a case by case basis due to the spatial/temporal variability of water and mis-matches between radiosonde locations and the AIRS field of view. However in a large statistical sample of these comparisons the random errors can be greatly reduced.

- It may also be possible to validate the instrument model, and some relative aspects of the spectroscopy, by examing the radiance residuals between radiances computed using the Level 2 retrieved profile and observed radiances. The wavenumber dependence of the residuals may highlight slowly varying spectroscopy errors. Instrument model errors (such as incorrect placement of the entrance slit aperture filter fringes) may also be inferred as follows. Perform a series of Level 2 retrievals, each using forward models with different placements of the entrance filter fringe peaks. Then examine the radiances residuals (computed for all channels) as a function of the fringe placement in the forward model and look for patterns that follow the known wavenumber dependence of the fringes. This process would be quite slow since it would most likely require use of kCARTA as the forward model. However, this may be the only way to validate the calibration of the fringe positions.

The AIRS channel center frequencies and the position of the entrance slit aperture filter fringes will not be determined until AIRS is in-orbit. Consequently the AIRS-RTA will not be using the proper instrument model at launch and must be re-computed post-launch once these quantities are determined. This process must be completed as quickly as possible to provide the Level 2 retrieval algorithms with an accurate forward model for the operational products. We will attempt to do as much Level 1B radiance validation as possible during this time frame (using kCARTA) so that the quick production of the new AIRS-RTA will also include any improvements to the spectroscopy and fast model parameterization.

Figure 2 is a more detailed diagram of Level 1B radiance validation. It pictorially shows how the instrument model, spectroscopy, and atmospheric profile information flow into the main validation activity, the analysis of radiance residuals. Note that validation of the AIRS-RTA is done with kCARTA radiances convolved with the instrument SRF model, and does not require observed AIRS radiances. This step does need to use actual observed (retrieved) AIRS profiles to ensure that a proper statistical set of profiles was used in the development of the AIRS-RTA. The arrows leading to the instrument model from the Level 1A/1B data are calibration activities, and are included here to emphasize that the instrument model will not be complete until AIRS is in orbit.

4.1 Validation of Radiances Sensitive to Upper Tropospheric Water Vapor

Although Level 1B validation may be successful for many AIRS channels, we expect it will be quite difficult to validate channels sensitive to upper tropospheric humidity, which is very difficult to measure accurately with radiosondes. This will affect a large number of water channels on the M3, M4a and M4b arrays because even if their weighting functions peak at lower altitudes, they have tails at higher altitudes where the radiosonde measurements are extremely inaccurate. Upper tropospheric water radiances are (1) quite low (220 -250K), and (2) offset significantly from the AIRS OBC temperature of 308K and thus are more subject to detector non-linearity errors than other channels. The combination of these problems will make validation of upper tropospheric water vapor radiances difficult. However, the importance of these channels for global climate change and outgoing longwave radiation (OLR), and the fact that AIRS will provide measurements of this key quantity that are far better than existing techniques, should provide impetus for a significant validation effort.

There are two possible approaches to overcome the limitations of the radiosonde network for validation of upper troposheric water radiances. First, an intensive field campaign is needed that stresses clear sky conditions and has the capability to make in-situ high-altitude water vapor measurements. Since it is difficult for the ER-2 to fly over a range of altitudes needed for in-situ water vapor measurements, our goals would be better served with NASA's WB57 equipped with several in-situ water sensors. Secondly, deployment of a water vapor lidar at a high altitude site, coupled with a microwave radiometer for measurement of the total water burden, could provide validation of upper tropospheric water vapor. A possible candidate site for this lidar would be NOAA's Mauna Lao observatory in Hawaii. Although there are existing lidars at some ARM sites, they have difficulty measuring high altitude water vapor due to the large signal reduction by the intervening lower atmosphere.

File translated from TEX by TtHgold, version 2.50.
On 9 Dec 1999, 17:16.